Electronic Thesis and Dissertation Repository

12-11-2013 12:00 AM

The Hippocampus Participates in a Pharmacological Rat Model of Absence Seizures

Justin Andrew Arcaro, *The University of Western Ontario*

Supervisor: Dr. Stan Leung, *The University of Western Ontario*
Joint Supervisor: Dr. Seyed Mirsattari, *The University of Western Ontario*
A thesis submitted in partial fulfillment of the requirements for the Master of Science degree in Neuroscience
© Justin Andrew Arcaro 2013

Follow this and additional works at: https://ir.lib.uwo.ca/etd

☀ Part of the Molecular and Cellular Neuroscience Commons

THE HIPPOCAMPUS PARTICIPATES IN A PHARMACOLOGICAL
RAT MODEL OF ABSENCE SEIZURES

(Thesis format: Monograph)

by

Justin Arcaro

Graduate Program in Neuroscience

A thesis submitted in partial fulfillment
of the requirements for the degree of
Master of Science

The School of Graduate and Postdoctoral Studies
The University of Western Ontario
London, Ontario, Canada

ABSTRACT

The thalamocortical network is responsible for the generation of spike-and-wave discharges (SWDs) in absence epilepsy. Recent studies suggest a potential involvement of the hippocampus, which may explain the variability in the extent of cognitive deficits among patients with absence epilepsy. I hypothesize that the hippocampus may become entrained in spike-and-wave discharges following thalamocortical activation. The gamma-butyrolactone (GBL) rat model of absence seizures was used in this thesis. Following GBL injection, SWDs of 4 to 6 Hz developed in the spontaneous local field potentials (LFPs) recorded by depth electrodes in the thalamus, neocortex and hippocampus. Synchronization of hippocampal, thalamic and neocortical SWDs was revealed by coherence analysis of the LFPs, and multiple unit activity of hippocampal neurons occurred within 250 msec prior to the negative peak of thalamic SWDs. Functional magnetic resonance imaging (fMRI) demonstrated functional connectivity between the hippocampus and the thalamocortical network. Thus, electrophysiological and fMRI activity of the hippocampus were shown to be time-locked to the thalamocortical SWDs, suggesting functional connectivity of the hippocampus and thalamocortical network during GBL-induced absence seizures.

Keywords: spike-and-wave discharges, absence epilepsy, gamma-butyrolactone, local field potentials, functional magnetic resonance imaging, functional connectivity, thalamocortical network

ACKNOWLEDGEMENTS

TABLE OF CONTENTS

LIST OF FIGURES & TABLES

FIGURES

TABLES

1.0 INTRODUCTION

1.1 EPILEPSY & SEIZURES

Epilepsy is a general classification of symptoms arising from abnormal brain function that affects up to 1% of the general population (Kadir & Chadwick, 1999). Seizures are the primary symptom of epilepsy, which are temporary disruptions of the brain with excessive, abnormal discharges synchronized throughout localized or distributed clusters of neurons. It is important to recognize a seizure only as a symptom of brain dysfunction and not as its own neurological condition because the healthy brain can be made to generate a seizure through a variety of insults including the use of drugs or trauma to the head. The various symptoms of epilepsy are classified into epilepsy syndromes defined as chronic neurological disorders characterized by recurrent, unprovoked seizures (Engel, 2001), and may be accompanied by behavioural manifestations such as altered consciousness, automatisms and sometimes tonic-clonic movements (International League Against Epilepsy, 1989). Since epilepsy is marked by the presence of spontaneous seizures, this suggests that in addition to temporary processes that take place during a seizure, there are alterations in the brain that predispose it to seizures and potentially disturb normal brain function (Lothman, 1993).

The vulnerability of the brain to seizure onset may be caused by a chronic pathological, structural or metabolic condition, and in many cases epilepsy is genetic (Berg et al., 2010; Berg & Scheffer, 2011). A seizure may initiated by the imbalance of excitatory and inhibitory neurotransmitters. Both increased excitation and decreased inhibition of neuronal activity can result in hyperexcitability of neuronal circuits. Perturbations at any of several levels of brain function may result in excessive neuronal

firing within networks of interconnected neurons. This includes excessive or insufficient release of specific neurotransmitters or alterations in interactions with their receptors (Stafstrom, 1998).

1.1.1 Classification of Seizures

The International League Against Epilepsy broadly classifies epileptic seizures as focal or generalized, depending on the location of origin and pattern of spread throughout the brain. The clinical manifestations of a seizure depend on the specific region and extent of brain involvement. Focal seizures originate within networks limited to one hemisphere and are either discretely localized or more widely distributed, with clinical manifestations based on the area of brain involved and the extent to which the discharges spread from the focus (International League Against Epilepsy, 1981). Generalized seizures originate at some point within the brain and rapidly engage bilaterally distributed networks, which may include cortical and subcortical structures, but may not necessarily include the entire cortex (International League Against Epilepsy, 1981). Manifestations of a generalized seizure can range from brief loss of awareness, which is characteristic of absence seizures, to rhythmic jerking of the extremities accompanied by loss of posture and consciousness, which are classified as generalized tonic-clonic seizures (Berg et al., 2010).

1.1.2 Absence Seizures

Absence epilepsies account for 15-30% of all epilepsy cases (Jallon & Latour, 2005). Absence seizures are generalized, are treated by specific antiepileptic drugs and

have a characteristic electroencephalographic (EEG) pattern. They make up the primary seizure type in a number of different absence epilepsy syndromes, including childhood absence epilepsy (CAE) and juvenile absence epilepsy (JAE) (ILAE, 1989). Absence seizures normally manifest between the ages of 4 years and adolescence, although they may occur at either ends of this age spectrum and roughly 65% of cases occur in females (Durá Travé & Yoldi Petri, 2006). Characteristics of absence epilepsy types include abnormal interictal EEG, usually normal and developmental status (Khan et al., 2012), and multiple seizure types. The primary seizure type is typical absence seizures, which occur with bilaterally synchronized 3 Hz spike-and-wave discharges (SWDs). These SWDs consist of burst discharges during the spike interspersed with inhibition during the wave (Steriade et al., 1994). Absence seizures are characterized by a brief loss of awareness with an abrupt onset and offset, with an average duration of two to ten seconds. Atypical absence seizures are less common. They occur with irregular spike-and-wave complexes, are associated with a higher incidence of changes in postural tone (ILAE, 1981), may be experienced with automatisms and are more associated with severe cognitive impairment (Holmes et al., 1987).

EEG is the primary means of recording electrical activity of the brain and for diagnosis of epilepsy, in which electrodes are strategically placed on the scalp of the patient to record neuronal activity. Voltage changes generated in cortical neurons are recorded as waveforms of various frequencies and amplitudes. Patterns vary according to the type of seizure and regions of the brain involved. Whereas the frequency of the atypical absence seizure is slower than 2.5 Hz, the specific EEG frequency recorded in a patient experiencing a typical absence seizure is 3-4 Hz and is detected in bursts of

bilaterally synchronous SWDs on a normal EEG background (Gastaut, 1970). Although slightly faster in frequency, SWDs can also be recorded from several animal models of absence seizures, including the monkey, rat and cat (**Figure 1**). This EEG pattern reflects the hypersynchronous activity among interconnected neurons of the thalamocortical (TC) network.

Absence seizures can be treated with ethosuximide, trimethadione, valproic acid or benzodiazepines (Vrielynck, 2013). Valproic acid is usually the first choice for treatment because it can control myoclonic jerks and tonic clonic seizures, which are occasionally associated with absence seizures (Khan et al., 2012). Some antiepileptic drugs actually exacerbate absence seizures, such as phenytoin, barbiturates and carbamazapine (Snead et al., 1999). Ethosuximide also has good efficacy and its anticonvulsant action is specific for absence epilepsy. Although poorly understood (Coulter et al., 1989), characterisation of the cellular mechanism of action is important for our understanding of the pathogenesis of absence seizures and can help in the development of other antiepileptic drugs.

1.2 NEUROBIOLOGY OF THE THALAMOCORTICAL NETWORK

1.2.1 Neurotransmitters

Glutamate and gamma-aminobutyric acid (GABA) are two neurotransmitters that mediate excitatory post synaptic potentials (EPSP) and inhibitory postsynaptic potentials (IPSP), respectively. EPSPs summate to depolarize the neuron and if there is a large enough depolarization, the cell generates an action potential. IPSPs hyperpolarize the cell, which prevent the neuron from firing an action potential.

A.

B.
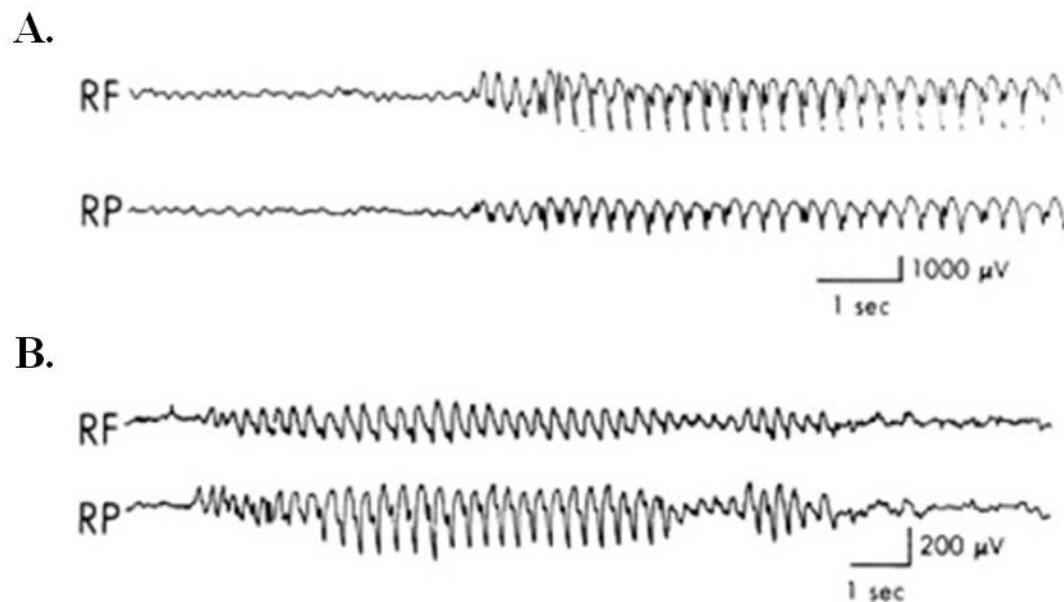
Figure 1. *Traces of electroencephalographic spike-and-wave discharges in the human and feline.* **(A.)** Sample traces of electroencephalographic recording from two surface electrodes placed on the scalp of a 9-year-old boy with childhood absence epilepsy showing typical 3-4 Hz spike and wave discharges. This brain pattern was accompanied by brief staring and behavioral arrest. **(B.)** Following penicillin injection, the feline model of absence seizures also demonstrates similar electrographic recordings and behavioural episodes. (RF: right frontal cortex, RP: right parietal cortex) (Adapted from Blumenfeld, 2003).

There are two types of excitatory glutamatergic receptors and activation of either of these leads to depolarization of the neuron as a result of positively charged ion influx. The N-methyl-D-aspartate (NMDA) receptors allow calcium, sodium and potassium ions to flow into the cell and require both the NMDA binding site and a glycine binding site to be occupied in order to activate the ion channel coupled to the receptor (Dingledine et al., 1999). Furthermore, the channel associated with the NMDA receptor is normally blocked by magnesium ions, which is only alleviated if the cell is sufficiently depolarized. These receptors are strongly voltage-dependent, a property not shared by non-NMDA or GABA receptors. When the ion channels coupled to the non-NMDA

receptors are activated, there is an influx of sodium and potassium ions, resulting in a depolarization of the cell. If the depolarization is sufficient enough to remove the magnesium ion from the NMDA-associated channel, NMDA-channel opening would result in a larger depolarization of the cell (Lothman, 1993).

GABA is the primary inhibitory neurotransmitter in the central nervous system. It is capable of activating two major types of receptors, the ligand-gated $GABA_A$ receptor and G protein-coupled $GABA_B$ receptors. $GABA_A$ receptors are ionotropic, ligand-gated ion channels and when GABA binds to $GABA_A$ receptors, associated ion channels enable negatively charged chloride ions to flow into the neuron. They form a pentameric assembly out of a possible 19 subunits, generally as a combination of α, β and γ subunits as the core, providing different functional properties (Connelly et. al., 2013). They induce a fast inhibitory IPSP that acts for 150 ms or less. In comparison, $GABA_B$ receptors are metabotropic, heterodimeric, G-protein coupled receptors that are coupled to channels that permit positively charged potassium ions to flow out of the cell (Benke et. al., 2012). $GABA_B$ receptors elicit IPSPs of 150-500 ms, which is relatively long in duration and therefore contribute to synaptic plasticity. Activation of either receptor may result in hyperpolarization, which inhibits neuronal firing (Lothman, 1993). However, it has been known that $GABA_A$ receptors may mediate depolarizing excitatory effects in immature neurons (Stein & Nicoll, 2003).

$GABA_B$ receptors are known to be active in the pathogenesis of absence seizures (Crunelli & Leresche, 2002). Studies have demonstrated that $GABA_B$ receptor agonists exacerbate absence seizures in experimental animal models and this exacerbation is much more potent than $GABA_A$ receptor agonists (Liu et al., 1992; Snead, 1992). Furthermore,

GABA$_B$ receptor antagonists have been shown to block absence seizures (Banerjee & Snead, 1995; Hu et al., 2000; Snead et al., 1999) and the EEG features that manifest from the abnormal interconnected circuitry of the thalamocortical network.

1.2.2 Principal Neurons of the Thalamocortical Network

The thalamus is the major relay station for afferents to the cortex. Messages from many different sources pass through the thalamus including messages from peripheral sense organs, other brain regions and the cortex itself (Sherman & Guillery, 2002). The primary thalamic inputs originate from sensory receptors, the cerebellum and the basal ganglia. Thalamic nuclei have strong reciprocal connections with the cortex (Deschênes et al., 1994), forming thalamo-cortico-thalamic circuits, which are responsible for specific systems such as auditory, somatic and visual systems.

The basic thalamocortical network is composed of three principal types of neurons: thalamocortical relay neurons, corticothalamic neurons and thalamic reticular neurons. The fundamental organization (**Figure 2**) consists of excitatory corticothalamic neurons with axons that project subcortically from pyramidal neurons of cortical layer VI into the thalamus and synapse onto both relay and reticular neurons (Blumenfeld, 2005). Relay neurons are also excitatory and their axons project to cortical layers III-IV as well as to dendrites of layer V-VI pyramidal cells. Relay neurons vary significantly in size, which is correlated with the depth to which they project into the cortex. These neurons are limited in their outputs and seem to only connect to the cortical layers and the reticular neurons. Reticular neurons however, are highly interconnected and have their own intrinsic oscillatory properties (Cavdar et al., 2008). They are GABAergic and are

capable of inhibiting thalamocortical activity via their direct connections with the relay neurons. The balanced inhibitory and excitatory effects of neurotransmitter release between thalamocortical neurons is of fundamental importance in controlling states of arousal, however altered neurotransmitter regulation can contribute to the development of absence seizures.

The thalamus is capable of initiating network oscillations yet the intrathalamic network is considerably more intricate than simple neuron-to-neuron inhibitory and excitatory communication. An important mechanism for producing inhibitory shaping of excitatory communication from thalamocortical and corticothalamic neurons is through a pattern of inhibitory connections that mediates feed forward inhibition (Crandall & Cox, 2013). The corticothalamic neuron synapses onto the dendrites of both reticular and relay neurons and generates EPSPs, however the reticular neuron has an inhibitory dendrodendritic synapse onto the relay neuron. Therefore the cortex excites the reticular neuron, which inhibits the thalamic relay cells via feed-forward inhibition. By restricting the excitation of relay neurons, this serves to enhance sensitivity to changing stimulation to perform temporal differentiation on changing sensory states (Koch & Ullman, 1985).

1.2.3 Reticular Thalamic Nucleus

The reticular thalamic nucleus is positioned between the thalamus and cortex and its individual neurons mediate selective attention under the influence of corticothalamic inputs. It forms a shell that surrounds much of the dorsal and lateral extent of the thalamus and is uniquely situated to influence the flow of information by controlling neural oscillations (Pinault, 2004). Oscillations within the TC network rely on the
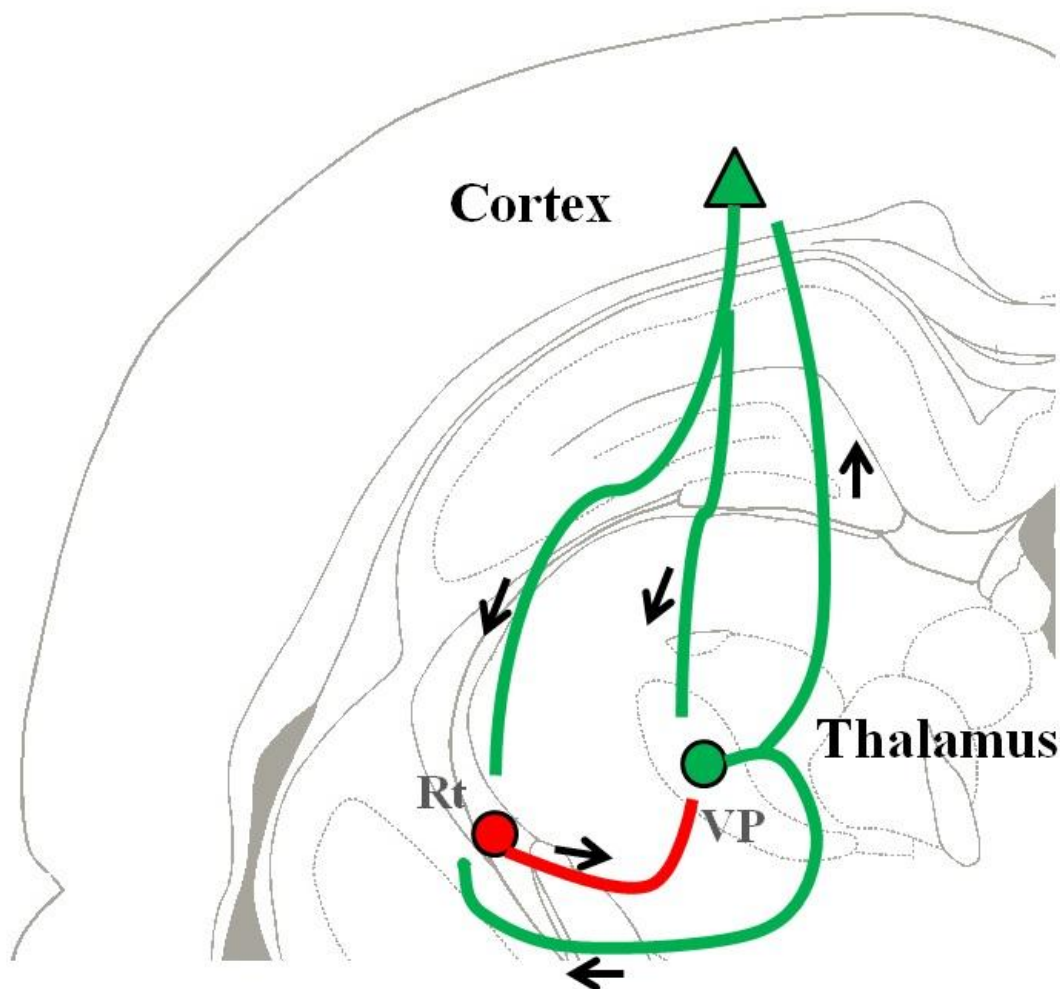
Figure 2. *Schematic diagram of the principal neurons of the thalamocortical network.* Shown is a coronal section through the right hemisphere of the rat brain. An example of a fundamental circuit in the thalamocortical network is demonstrated. The pyramidal cells of the cortex (green triangle) project subcortically into the thalamus onto the reticular thalamic nucleus (Rt, red circle) and onto principle relay nuclei (green circle). The ventroposterior (VP) complex is the example principal thalamic relay nucleus used here. Relay neurons project back up into the cortex as well as onto reticular thalamic neurons, which have reciprocal projections back onto relay neurons. Red neurons are GABAergic, green neurons are glutamatergic.

intrinsic oscillatory properties of the reticular neurons which regulate states of arousal (Steriade & Llinás, 1988). Tonic firing of the reticular neurons allows for faithful signal transmission from the external environment to the cortex (Deleuze et al., 2012) during

wakefulness and manifests as desynchronized EEG. Conversely, rhythmic burst firing of the reticular neurons dampens communication to the cortex during altered states of consciousness (Cheong & Shin, 2013) and manifests as highly synchronized neuronal activity on EEG recordings. These response modes depend on the status and distribution of specific ion channels within thalamic neurons.

1.2.4 T-Type Calcium Ion Channels

Ion channels differ with respect to their structure, the number of subunits they are composed of and the way in which they are regulated. A major function is to control the flow of ions across the neuronal membrane to establish a resting membrane potential, which shapes action potentials and ultimately communication between neuronal networks of the brain (Jones, 2007). Most generalized epilepsies have complex inheritance patterns, however a few have a Mendelian inheritance pattern associated with single-gene mutations found in ion-channel proteins (Chang & Lowenstein, 2003). One of the primary ion channels of interest in the study of absence seizures and the thalamocortical network is the calcium ion channel. Calcium ions have a dual role in neurons, as modulators of neuronal firing pattern and as intermediates in cellular activities such as neurotransmitter release or enzyme metabolism. They are unique because calcium acts as a second messenger, so when it enters the cell it will influence numerous physiological functions such as gene expression and neurotransmitter release (Fliegert et al., 2007).

Most calcium channels are activated when the membrane potential is more positive than -40mV and are termed high-voltage activated (HVA). These include the currents I_L, I_N, I_P, I_Q, and I_R. The HVA currents are important to allow calcium ions to

enter the cell in order to activate calcium-dependent potassium currents. The activation of these currents then modifies action potentials generated in the cell (Sah & Faber, 2002). Low-threshold calcium currents are activated at near the resting membrane potential (Andersen and Sears, 1964) and are termed low-voltage activated (LVA). The discovery in thalamic neurons of specific T-type calcium ion channel currents (I_T) (Deschênes et al., 1984) made basic research on absence seizures shift to focus on the role of the thalamus. The T-type calcium current is involved in the generation of rhythmic burst firing and is characterized by a threshold of activation at -65 mV (Talley et al., 2000), which is below the threshold of typical sodium-potassium dependent action potentials around -55 mV.

Influenced by reticular neurons and their mode of firing, relay neurons possess T-type calcium channels and therefore also possess a unique ability to switch their mode of responsiveness in a way as to contribute to network oscillations (Talley et al., 1999). When neurons are depolarized, T-channels are inactivated. GABA from reticular neurons activates $GABA_A$ and $GABA_B$ receptors on relay neurons, generating an IPSP. IPSPs can result in membrane hyperpolarization, which may be just enough to remove inactivation (de-inactivation) of the T-type calcium channels, generating bursts of action potentials as a form of post-inhibitory rebound and is termed a calcium-dependent low-threshold spike (LTS) (Perez-Reyes et al., 1998). De-inactivation of T-type calcium channels ensures that the bursting output of relay neurons is transmitted to the cortex and directly to the reticular neuron as synaptic excitation, thus renewing the continuous communication among the principle neurons of the thalamocortical network (Huguenard & Prince, 1994). This network oscillation thus depends on reciprocal connectivity

between excitatory and inhibitory neurons and an LTS generated by T-type calcium ion channels.

1.3 THE ROLE OF THE THALAMOCORTICAL NETWORK IN ABSENCE SEIZURES

All thalamic relay cells respond to excitatory inputs in two distinct ways, which are burst and tonic firing, and these response modes reflect the status of I_T (Destexhe et al., 1998). These responses allow the thalamus to provide relay that affects the nature and format of information reaching the cortex, which is why the thalamus is considered to be the gateway of information processing in the brain. The active waking state with eyes open is more associated with a maintained depolarization of thalamic relay cells resulting in the inactivation of low-threshold calcium currents and the tonic firing mode. This is associated with a desynchronized EEG pattern, which allows for faithful signal transmission from the external environment through the thalamus and to the cortex (Sherman, 2001).

The burst firing mode is characterized by synchronization across populations of relay neurons. During slow-wave sleep (Steriade et al., 1993), the membrane potential of these neurons is hyperpolarized, resulting in the removal of inactivation of the low-threshold calcium current. This allows these cells to generate bursts of two to five action potentials (**Figure 3**). The large population of relay neurons that burst at the same time gives rise to synchronized activity in the form of sleep spindles that can be recorded from the scalp using EEG. This system can be altered resulting in the development of SWDs of absence seizures, which are heavily dependent on specific GABA receptor activation.

-65 mV

-75 mV

40 mV

80 ms

Tonic Firing **Burst Firing**
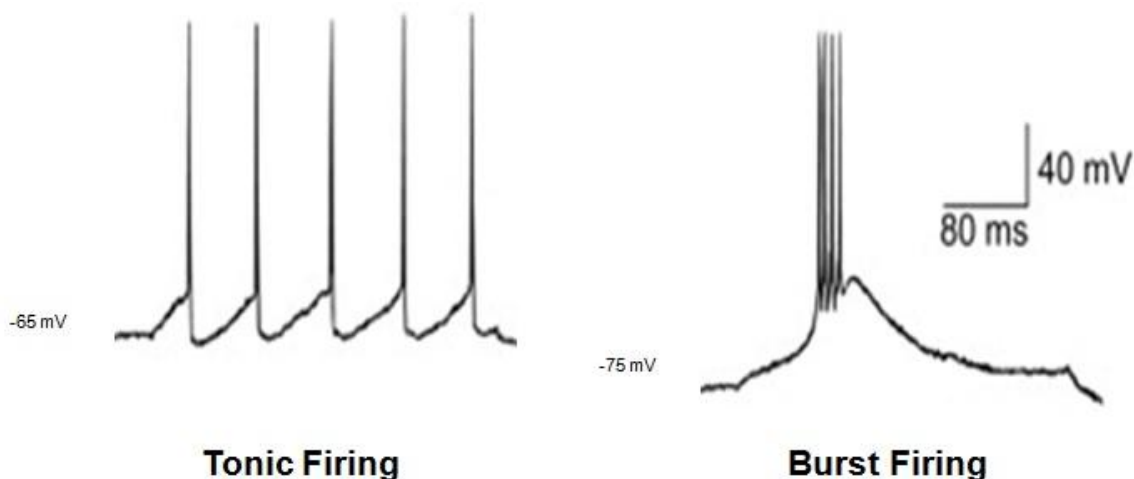
Figure 3. *Thalamocortical neurons generate two distinct firing response modes, which depend on T-type calcium ion channels.* Shown are two recordings from a thalamic relay neuron. Depolarization of thalamic relay neurons, and thereby inactivation of I_T, results in the generation of a train of action potentials if the membrane potential is more positive to -65 mV (left). When the membrane potential is at or negative to -75mV (right), I_T is de-inactivated, resulting in the generation of bursts of action potentials (calcium-dependent low-threshold spike). Changes in these modes can regulate synchrony in such a way as to switch to burst firing mode under pathological conditions associated with absence epilepsy. (Adapted from Zhan et al., 1999; McCormick & Pape, 1990)

GABA can activate $GABA_A$ and $GABA_B$ receptors, both present within the thalamocortical network. Countering the synchronizing influences is an inhibitory effect by interneurons of the reticular thalamic nucleus, termed collateral inhibition (Bal et al., 1995). This inhibition is mediated by an isoform of $GABA_A$ receptors composed of α3, β3 and γ2 subunits. The activation of anti-oscillatory $GABA_A$ receptors appears to prevent the development of uncontrolled hypersynchronous oscillations by inhibiting the excitation of surrounding reticular neurons (Huguenard & Prince, 1994). In comparison, pro-oscillatory communication between reticular neurons and relay neurons is mediated by $GABA_A$ receptors composed of α1, β2 and γ2 subunits (Sohal et al., 2003). Activation

of pro-oscillatory GABA$_A$ receptors maintains synchronized neural activity by activating T-type calcium channels in relay neurons essential for feedback to reticular neurons.

The differential activation of GABA$_A$ and GABA$_B$ receptors is responsible for the ability to switch between thalamocortical states, and is also an important determinant of the hypersynchronous neural activity involved in absence seizures (Huguenard & McCormick, 2007). Using thalamic slices in the ferret (**Figure 4**), it was demonstrated that GABA$_A$ antagonists block normal 6-10 Hz oscillations, producing spike-and-wave-like 3 Hz oscillations and suggesting that the thalamocortical neurons may become vulnerable to seizure-like activity in the absence of normal GABA$_A$ receptor function (Blumenfeld & McCormick, 2000). In comparison to the 100 ms IPSPs generated by GABA$_A$ receptors, those generated by GABA$_B$ receptors have a longer duration of 300 ms and larger hyperpolarization, which may enhance the de-inactivation of T-type calcium channels in relay neurons, thereby resulting in large rebound bursts of action potentials (Bal et al., 1995). The same study demonstrated that the blockade of GABA$_B$ receptor activation during various intensities of artificial cortical input leads only to the generation of normal 6-10 Hz spindle oscillations and prevents the 3 Hz spike-and-wave-like discharges. These findings suggest that enhanced cortical firing onto the thalamus generates slow IPSPs and spike-and-wave-like activity by promoting GABA$_B$ receptor activation.

In summary, in the presence of enhanced cortical input, reticular neurons release GABA, which induces slow GABA$_B$ receptor mediated IPSPs resulting in hyperpolarization of the relay neuron. This hyperpolarization de-inactivates T-type calcium channels, causing rebound bursts of action potentials to contribute to
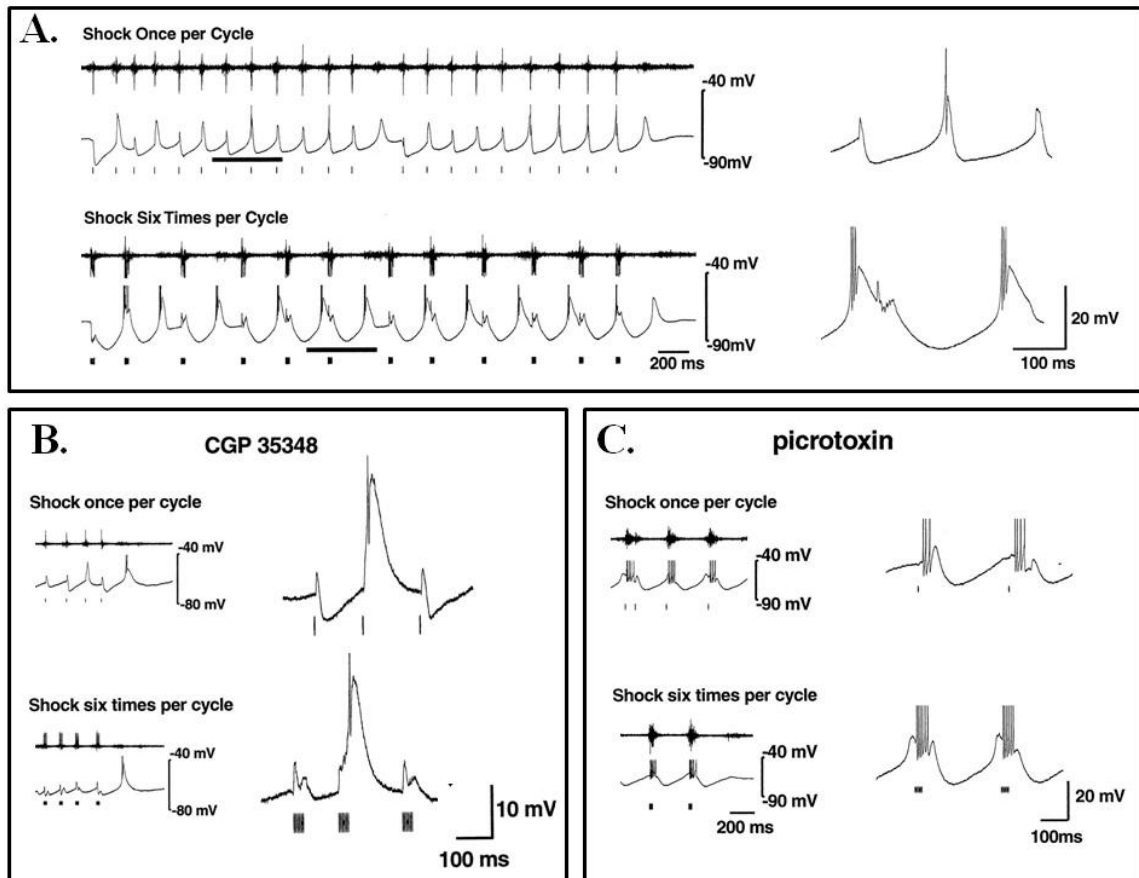
Figure 4. *Differential GABA$_A$ and GABA$_B$ receptor activation play a role in thalamocortical oscillations.* A stimulator was set to deliver either one shock or brief 200 Hz bursts of six shocks simulating the cortical input onto ferret thalamic slices. Stimulus pulses are represented by tick marks below each trace. Extracellular (top traces) and intracellular (bottom traces) recordings from thalamic relay neurons are shown in the presence of one or six shocks. Expanded traces of the intracellular recordings are shown to the right. **(A.)** With cortical stimulation of one shock, the network generated 6-10 Hz oscillations with fast IPSPs and brief rebound bursts in thalamocortical cells that resemble normal rhythms. With higher frequency cortical stimulation, the network transformed to 3-4 Hz activity, with slow IPSPs and rebound burst firing as demonstrated in the trace to the right. **(B.)** Local application of the GABA$_B$ receptor antagonist CGP 35348 had no effect on the 6-10 Hz oscillation and only produces fast IPSPs and brief rebound bursts in the thalamocortical cells under one shock stimulation. However, application of CGP 35348 eliminated the 3-4 Hz activity in the presence of six shock stimulations and also produced fast IPSPs. **(C.)** The GABA$_A$ receptor antagonist picrotoxin blocked 6-10 Hz oscillations and fast IPSPs under one shock stimulation, and now only elicited slow IPSPs, large rebound bursts and 3-4 Hz oscillations. Using six shocks, picrotoxin elicited no change in the thalamocortical neuron. This study is important because it demonstrates that enhanced cortical input to the thalamus causes 3-4 Hz oscillations via GABA$_B$ receptor activation. (Adapted from Blumenfeld & McCormick, 2000)

hypersynchronized thalamocortical oscillations, which may manifest as SWDs. It is probable that the differential activation of $GABA_A$ and $GABA_B$ receptors, the activation of T-type calcium channels and the ability of principle thalamocortical neurons to switch mode of firing, all contribute to the shift from normal to paroxysmal discharges of absence seizures. Although absence epilepsy is known to be $GABA_B$ dependent, it is unknown whether or not cortical input to the thalamus is solely responsible for $GABA_B$ activation and how cortical firing becomes enhanced in the first place. Dynamic changes within the circuitry can regulate synchrony in such a way as to allow thalamocortical circuits to be used under pathological conditions such that they instead generate hypersynchronous epileptic discharges associated with generalized absence epilepsy.

1.3.1 Competing theories on the pathophysiology of absence seizures

In 1941, Herbert Jasper analyzed EEG of patients with absence seizures. No evidence was found for a cortical origin, so it was proposed that seizures had a subcortical origin (Jasper & Kershman, 1941). Later, Jasper established the first experimental model of a spike-wave pattern by stimulating the thalamus, providing support for the existence of a subcortical involvement. Behavioural arrest of human absence seizures could be mimicked in cats by 3 Hz intralaminar thalamic stimulation (Hunter & Jasper, 1949). The thalamus became referred to as the central pacemaker for generalized discharges, however debate began as to whether the thalamus or the cortex was the driver of discharges. According to several investigators, the expression of generalized seizures was due to a cortical focus, which then spreads to involve the thalamus (Luders et al., 1984). Using the feline penicillin model of human absence

epilepsy, it was demonstrated that phase-locked firing started a few cycles earlier in the cortex as opposed to the thalamus, suggesting that the paroxysmal oscillation is initiated in the cortex which then entrains the thalamus (Avoli & Gloor, 1981; Avoli et al., 1983). This is known as the corticoreticular theory, which is the most widely accepted of the absence theories today, however there is still debate as to the relationship between the thalamus and cortex.

To elucidate these neural networks, thalamic and cortical lesions were conducted in epileptic WAG/Rij rats, which demonstrated that an intact cortex is required for spike-and-wave generation and that the intrathalamic circuitry alone is not sufficient for the generation of spike-and-wave discharges (Meeren et al., 2002). In studies recording simultaneous local field potentials (LFPs) in the cortex and thalamus, nonlinear association analysis of spike-wave discharges showed a consistent cortical focus in the perioral region of the somatosensory cortex throughout the seizure (Pijn et al., 1990). SWDs recorded in other cortical sites lagged behind this focus with time delays that increased with electrode distance. Furthermore, the first 500 ms of the seizure was led by the cortex and then followed by its thalamic counterpart. This suggested that once the oscillation has been set in motion by the cortex, the cortex and thalamus form an oscillatory network in which both structures drive each other, thereby maintaining rhythmic discharges. This cortical focus theory bridges both cortical and thalamic theories (Meeren et al., 2005).

For years, animal models of absence epilepsy have been extremely useful in understanding the generation of SWDs, cortical and thalamic involvement, and pharmacological properties. Animal models are still very useful, especially with the

development of neuroimaging techniques, including functional magnetic resonance imaging (fMRI). These developments not only allow investigators to look at the thalamocortical interactions, but now permit the investigation of all structures of the brain involved in absence seizures.

1.4 RODENT MODEL OF TYPICAL ABSENCE SEIZURES

With the advent of a number of animal models of generalized absence seizures, the controversy between which structure – the cortex, the thalamus, or both - controls the bilaterally synchronous SWDs has been challenged. However, the availability of these models has advanced our understanding of the basic mechanisms of absence seizures. To be a valid investigative tool, an animal model of absence seizures should reflect clinical and pharmacological characteristics of the disorder. These criteria include reproducibility and predictability for experimental purposes. The EEG patterns and behaviour should be analogous to those of human absence seizures. Therefore there should be bilaterally synchronous SWDs associated with behavioural arrest with or without head drop and nystagmus. Further criteria, and perhaps most important, include attenuation of the SWDs by anti-epileptic drugs commonly used to treat human absence seizures (Snead 1999).

A commonly used acute model of absence seizures that meets the above criteria (Snead, 1988), and the one used in this thesis, is the gamma-hydroxybutyric acid (GHB) rat model (Snead et al., 1976; Godschalk et al., 1977). GHB is a natural metabolite of the brain where it is derived from the conversion of its parent neurotransmitter, GABA (Snead, 1989). It has been found in rat, cat, guinea pig and bovine brain at concentrations

of 1-4 nmol/g (Roth & Giarman, 1970) and is present in highest concentrations in the hippocampus, midbrain, diencephalon and cerebellum (Roth, 1970). GHB opposes the process of inducing endocytosis of the $GABA_B$ receptor thus prolonging the functionality of the receptor on the cell surface and accounts for the 30-40 minute half-life of the drug (Schep et al., 2012).

Evidence suggests that the GHB receptor is presynaptic and G-protein-coupled, however most of the physiologic and pharmacologic effects of systemically administered GHB are mediated by the $GABA_B$ receptor (Snead, 2000). GHB may act both directly as a $GABA_B$ receptor agonist and indirectly on the $GABA_B$ receptor through GHB-derived GABA. The supraphysiologic (millimolar) concentrations of GHB that result from systemic administration have been found to compete for binding sites at the $GABA_B$ receptor and have an electrophysiological effect that is blocked by a specific $GABA_B$ receptor antagonist and not by a GHB receptor antagonist (Gervasi et al., 2003). The idea that $GABA_B$ receptor-mediated mechanisms are operative in the pathogenesis of absence seizures is also supported by the observation that a specific $GABA_B$ receptor antagonist blocks absence seizures in four different experimental models of absence seizures, including the GHB model (Hu et al., 2000). Conversely, the $GABA_B$ receptor agonist (-) baclofen, causes a marked exacerbation of absence seizures in the GHB model (Banerjee & Snead, 1995; Snead, 1992), to the point of absence status epilepticus which may last for hours.

GHB is a $GABA_B$ receptor agonist that initiates the cascade of events that lead to hypersynchronous oscillations in the thalamocortical network. When administered, GHB produces a predictable sequence of electrographic and behavioural events that resemble

that of human absence seizures (Snead et al., 1976). The GHB-treated animal shows an arrest of motor activity with fixed staring and occasional twitching of the vibrissae and facial muscles. Concomitant with these behavioural abnormalities, a 4-6 Hz spike-and-wave pattern is produced on the electroencephalograph, sometimes reported at 7-9 Hz (Snead et al., 1999). This model is also pharmacologically unique because it responds well to the common antiepileptic drugs used to treat human absence seizures (Snead, 1996) and does not respond well to phenytoin and carbamazepine, which are known to exacerbate human absence seizures (Liu et al., 2006).

The GHB model has a unique developmental profile which reflects the propensity of the developing brain for the occurrence of bilaterally synchronous SWDs. The developmental profile of human absence seizures is mirrored in the GHB rat model where the GHB-induced seizures are most pronounced at postnatal age of 3 to 4 weeks (Snead, 1992, 1995), indicating that maturation of the thalamocortical network is necessary for absence seizure activity. Furthermore, the ontogeny of the thalamocortical network in the rat parallels the responsiveness of the GHB model to antiepileptic drugs such as ethosuximide and these observations are consistent with the finding that rhythmic thalamocortical responses do not begin to develop in rats until postnatal day 12 and are not fully developed until the fourth postnatal week (Snead, 1994, 1995).

The use of gamma-butyrolactone (GBL), a prodrug of GHB, has been shown to enhance reproducibility and predictability of the GHB model and so GBL is used because of its consistency and rapidity of onset (Guidotti & Ballotti, 1970). GBL has no known pharmacological activity of its own (Giarman & Roth, 1964), so it must be cleaved by a lactonase present in the plasma and liver (Guidotti & Ballotti, 1970), which can then be

taken up from the blood by the brain as GHB (Roth & Giarman, 1966). When GBL is injected intraventricularly in the brain, there is no pharmacological action because the brain does not have the lactonase to hydrolyze it to GHB (Roth, 1970; Snead, 1991). GBL is administered intraperitoneally, particularly for use as a model of absence seizures.

The frequency and pattern of the SWDs observed in this model are quite similar to those of the genetic rodent models of absence seizures, WAG/Rij rats (van Luijtelaar & Coenen, 1986) and Genetic Absence Epilepsy in Rats from Strasbourg (GAERS) (Vergnes et al., 1982). Therefore the GBL model meets all criteria which have been put forth for experimental absence seizures. It is a useful experimental model for studying the mechanisms of bilaterally synchronous SWDs, the thalamocortical interactions and other networks involved in absence seizures.

1.5 CURRENT STUDY

The primary goal of absence epilepsy research is to understand the neuronal mechanisms that underlie synchronous oscillatory activity within interconnected thalamocortical networks. Imaging techniques have made it possible to study absence epilepsy at the network level while electrophysiology has provided insight into potential causes including perturbations in neurotransmitters and their receptors, as well as in various ion channels. However when investigating the basic mechanisms involved in absence seizures, it is important to remember that the thalamus and the cortex are widely interconnected with other neural networks. Imaging studies have demonstrated that brain

regions beyond the thalamocortical network are participating in some aspects of these seizures (Gotman, 2008).

The current study focuses on the potential involvement of the hippocampus. Although very few studies have investigated a role for the hippocampus, recent observations in models have pointed to a possibly important link between absence seizure mechanisms and limbic structures (Onat et al., 2013). The motivation to explore the hippocampus stems from the fact that, although not characteristic of all patients, some present with severe cognitive impairment and memory loss (Caplan et al., 2008). Furthermore the hippocampus receives prominent projections from the thalamus. The reticular thalamic nucleus serves as a gateway between specific thalamic nuclei and the hippocampus (Cavdar et al., 2008) in a similar manner it serves between the thalamus and the cortex.

The primary objective of the current study was to use electrophysiological techniques and functional imaging to investigate interactions between the thalamocortical network and the hippocampus in a model of absence seizures induced by GBL in rats. In the first series of experiments, local field potentials were recorded simultaneously in different brain areas, and analyzed by means of power and coherence spectral analysis. In the second experiment, multiple unit recordings were made at the hippocampal CA1 pyramidal cell layer to study the temporal relationship between hippocampal neuronal unit activity and GBL-induced SWDs. In a third experiment, fMRI during GBL-induced absence seizures was used to look at possible changes in the global alterations in functional connectivity amongst the thalamus, cortex and the hippocampus. This technique offers the advantage of studying functional connectivity between our regions of

interest with the rest of the brain. We hypothesized that the hippocampus may become entrained by thalamocortical SWDs.

2.0 MATERIALS & METHODS

2.1 Animals

Adult male Long-Evans rats (Charles River Laboratories) weighing 250-400 grams were used in these experiments. Rats were housed in standard cages in a temperature regulated environment in a 12:12hour light/dark cycle starting at 7 am with food and water freely available. All experiments were conducted during the day between 9 am and 7 pm. All experiments were carried out in accordance with the guidelines established by the Canadian Council on Animal Care and approved by the Animal Use Committee of Western University.

2.2 LOCAL FIELD POTENTIALS & NEURONAL UNIT EXPERIMENTS

2.2.1 Surgery & Electrode Implantation: Local Field Potentials & Behaviour

Recording electrodes were constructed out of stainless steel wire, 0.005 inches in diameter and were insulated with Teflon except at the cut tips. Eight rats were initially anesthetized with sodium pentobarbital (60 mg/kg, intraperitoneal (i.p.)) and secured in a stereotaxic frame. The skull was exposed with lambda and bregma in a horizontal plane. Burr holes were drilled for implantation using coordinates from a rat brain atlas (Paxinos and Watson, 2009). Rats were chronically implanted with depth electrodes at the following coordinates relative to bregma: right frontal cortex layer IV/V (anterior 1.4 mm, lateral 2 mm, ventral 1.5 mm), right ventrolateral thalamic nucleus (posterior 2.4 mm, lateral 2.2 mm, ventral 6.0 mm), right visual cortex layer IV/V (posterior 7.0 mm, lateral 3.0 mm, ventral 1.5 mm) and a depth electrode was positioned in the left CA1 region of the hippocampus (posterior 3.2 mm, lateral 2.2 mm, ventral 3.0 mm) and

another in the parietal cortex layer IV/V (posterior 3.2 mm, lateral 2.2 mm, ventral 1.5 mm). A jeweller's screw was secured over the left frontal cortex and over the left cerebellum to serve as recording grounds in all rats. The electrodes were fixed by creating a head cap made of acrylic cement. Experiments did not commence until at least a week within surgery for recovery.

2.2.2 Surgery & Electrode Implantation: Neuronal Unit Recordings in Relation to SWDs

Recording electrodes for the CA1 pyramidal cell layer were constructed out of stainless steel wire, 0.003 inches in diameter and were insulated with Teflon except at the cut tips. The thalamic electrodes were made of stainless steel wire of 0.005 inches in diameter. Six rats were initially anesthetized with sodium pentobarbital (60 mg/kg, i.p.) and secured in a stereotaxic frame. The skull was exposed with lambda and bregma in a horizontal plane. Burr holes were drilled for implantation using coordinates from a rat brain atlas (Paxinos and Watson, 2009). Rats were chronically implanted with a depth electrode in the right ventrolateral thalamic nucleus (posterior 2.4 mm, lateral 2.2 mm, ventral 6.0 mm) and bi-polar depth electrodes were implanted bi-laterally in the CA1 pyramidal cell layer of the hippocampus (posterior 3.2 mm, lateral 2.2 mm, ventral ~2.5 mm) using electrophysiological criteria (Leung, 1979). The individual stainless steel wires of the left bipolar electrode were cut at the same length and the wires of the right bipolar electrode were cut with a difference of 0.5 mm. A jeweller's screw was secured over the left frontal cortex and over the left cerebellum to serve as recording grounds in

all rats. The electrodes were fixed by creating a head cap made of acrylic cement. Experiments did not commence until at least a week from surgery for recovery.

2.2.3 Local Field Potential Recordings

Bench-top experiments were conducted to characterize the GBL model of absence seizures in freely moving rats. Each day for 1 week following surgery, rats were placed in a Plexiglas cage for 1-2 hours to become accustomed to the recording environment. On the day of the experiment, each electrode was connected to a Grass Electroencephalograph Model 8-10 system for EEG recordings. EEG was filtered between 0.3-70 Hz and sampled at 200 Hz by custom made software (Data Acquisition Software DAS 2.1, 1998), using a UEI WIN-30DS (United Electronic Industries, Watertown, MA) 16-channel data acquisition board. Once the rats habituated to the recording condition, baseline recordings were collected for 30 minutes during awake immobility. GBL (200 mg/kg) was then injected intraperitoneally and EEG was continuously recorded for 2 hours following injection.

2.2.4 Neuronal Unit Recordings in relation to Spike-and-wave Discharges

Activity in the CA1 pyramidal cell layer was recorded to characterize hippocampal neuronal unit activity in relation to the SWDs induced by GBL in the rat. Each day for 1 week following surgery, rats were placed in a Plexiglas cage for 1-2 hours to become accustomed to the recording environment. On the day of the experiment, each electrode was connected to a Grass 7P511 preamplifier. The hippocampal and thalamic EEG recording channels were filtered between 0.03 Hz and 3 kHz (first order bandpass

filter). For neuronal unit recordings, the hippocampal signal was further amplified by 500-1000 times and highpass filtered at 250 Hz (second order filter). EEG and unit signals were then fed into a Data Translation D303 analogue-to-digital converter and sampled and stored at 10 kHz by SciWorks 7 (DataWave Technologies, Loveland, CO, USA). Data acquisition and analyses were done by custom-made scripts written in SciWorks 7. Once the rats habituated to the recording condition, baseline recordings were collected for 30 minutes during awake immobility. GBL (200 mg/kg) was then injected intraperitoneally and EEG and neuronal units were recorded in 3 minute time intervals, continuously for 2 hours. During unit acquisition, the detection threshold of a neuronal unit was set to at least twice the amplitude of the background, which allowed the waveform (0.6 ms before and 0.6 ms after the detected peak) of all detected units to be stored during acquisition. Thresholds were kept constant for recordings in each rat.

2.2.5 Perfusion, Histology and Staining

Following experiments, rats were euthanized with 1 ml of sodium pentobarbital (60 mg/kg i.p.). The rats were intracardially perfused with 60 ml (x2) of saline followed by 60 ml (x2) of 4% formaldehyde solution. The brain was extracted from the cranium and placed in 4% formaldehyde solution until ready for sectioning. Brains were frozen and sliced on a Leitz 1320 freezing sledge in 60 μm coronal sections. Brain slices were mounted onto slides and later stained with thionin. The electrode placements for LFPs (**Figure 5**) and neuronal unit recording experiments (**Figure 6**) were identified and confirmed using a light microscope.
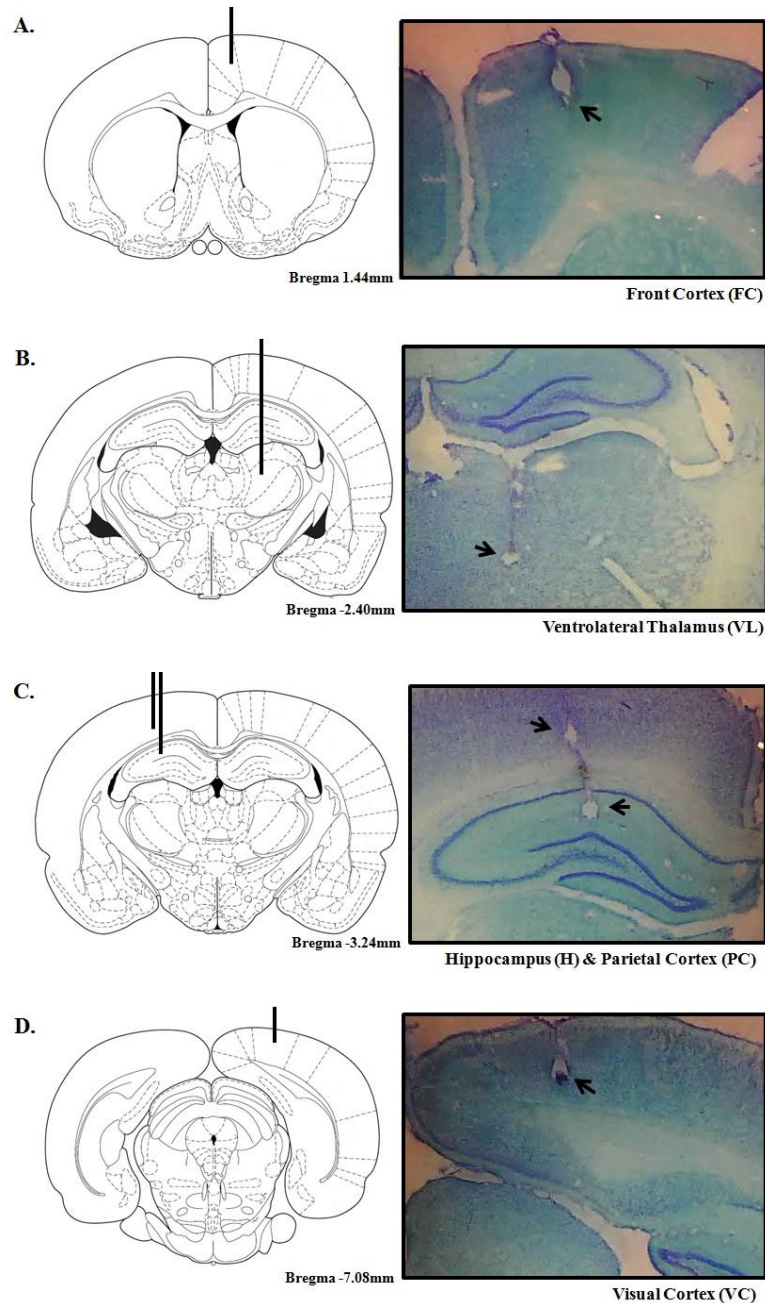
Figure 5. *Coronal rat brain slices indicating electrode placements for LFP and behavioural experiments.* Locations were based on coordinates taken from Paxinos and Watson (2009). Schematic slices on the left illustrate placements of recording electrodes (solid black line) and examples of corresponding placements (black arrows) in thionin stained sections are on the right. **(A)** Placement in the left frontal cortex (A1.4, L2, V1.5), **(B)** the left ventrolateral nucleus of the thalamus (P2.4, L2.2, V6.0), **(C)** two electrodes placed in the right CA1 region of the hippocampus (P3.2, L2.2, V3.0) and right parietal cortex (P3.2, L2.2, Ventral 1.5), and **(D)** the visual cortex (P7.0, L3.0, V1.5).
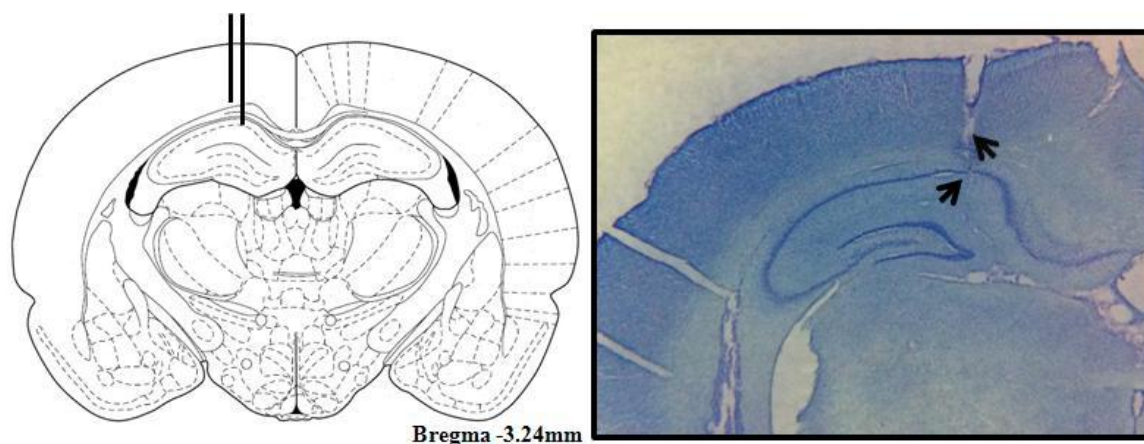
Figure 6. *Coronal rat brain slice indicating electrode placement for hippocampal neuronal unit recordings.* Locations were based on coordinates (CA1 pyramidal cell layer P3.2, L2.2, ~V2.4) taken from Paxinos and Watson (2009). Schematic slice on the left illustrates placements of the right hemisphere of bi-polar recording electrodes (solid black lines) and an example of corresponding placements (lower black arrow – CA1 pyramidal cell layer, upper black arrow – alveus) in a thionin stained section is on the right.

2.2.6 Data Analysis: Local Field Potentials & Behaviour

All EEG recordings were visually inspected for SWDs using a custom made program, Analysis Software Package 6.1.14. The first sign of SWDs following GBL injection was identified as the onset and this stage was identified as bursting SWDs because SWDs appeared in bursts on a normal EEG background. The second stage was identified as continuous SWDs and was characterized by the disappearance of both bursting SWDs and normal EEG background. Only high amplitude, continuous SWDs were present in this stage. Onset times were averaged using all 8 rats. EEG data were analyzed by a Matlab 7.0 program. Each EEG spectrum was constructed by averaging 6 or more segments of EEG, with each segment being 1024 points, or 5.12 s with 200 Hz sampling (Leung et al., 1982). Each segment was tapered (10% of segment at each end) by a cosine bell function, and the auto- and cross-power (coherence and phase spectra)

were obtained by Fast Fourier Transform and smoothed across 5 adjacent frequency bins, by an elliptical function. Each spectrum had a frequency resolution of 0.19 Hz (1/5.12 s), and statistically independent values were separated by 5 bins, or 0.95 Hz, but with more than 60 degrees of freedom. Peak power and coherence values and frequencies were obtained from the power and coherence spectra during bursting and continuous stages of SWDs. Statistical tests were performed In GraphPad Prism 4. Statistics were conducted on the average of these values using nonparametric Mann-Whitney U tests. The power in each placement was averaged between 2-6.5 Hz during baseline and stages of SWDs. Statistics were conducted on the integrated power using nonparametric Kruskal-Wallis tests and Dunns Multiple Comparison post-tests. Maximum coherence values were identified between 2-9 Hz after comparing coherence values for all possible pairs (10) of brain regions. Non-parametric Kruskal-Wallis tests and Dunns Multiple Comparison post-tests were conducted to determine significance.

2.2.7 Data Analysis: Neuronal Unit Recordings in relation to Spike-and-wave Discharges

All EEG and neuronal unit recordings were visually inspected for SWDs, and analyzed using a custom made program, written with SciWorks 7. One 3 minute file was chosen for each of baseline, bursting SWDs and continuous SWDs per rat. The file chosen for bursting SWDs and continuous SWDs were identified using the EEG patterns characterized in the behavioural studies. To identify the temporal relationship between hippocampal unit firing and thalamic SWDs, a threshold was set in the thalamic EEG recording to detect the negative peak of the SWD. Since the amplitude threshold was

fixed (Event Detection in SciWorks 7), the detection could occur on the rising phase of the peaks, and only the SWDs of near maximal peak amplitudes were detected. Files were replayed in SciWorks 7 to construct peri-event time histograms of the detected hippocampal neuronal units, the averaged EEG signals for thalamic and hippocampal SWDs and power spectra of the EEG. Power spectra were constructed based on Fast Fourier Transform of a 1 s segment of the EEG signals, and more than 20 segments were averaged to give an average spectrum. The resolution of the power spectra was 1 Hz, with Nyquist frequency of 500 Hz. The negative peak of the thalamic SWD was used as the event trigger (time zero), and 500 ms before and 500 ms after the event was the time period of the time histogram and averaged EEG signals. All data was exported to Excel for further analysis and plotting.

Time histograms of unit firing were constructed using 20-msec time bins. Each histogram was normalized by the total number of units detected throughout the 3 minute interval, to give a probability of discharge per bin. The 1000 ms histogram was divided into 4 intervals – T1 (-500 to -250 msec), T2 (-250 to 0 msec), T3 (0 to 250 msec), and T4 (250 to 500 msec). Within each rat nonparametric Kruskal-Wallis and Dunn's Multiple Comparison post-tests were conducted to test counts across all 4 segments and determine if neuronal firing was uniformly distributed across time. Each time segment was then tested across stages of GBL-induced SWDs to identify significant changes in peak-related firing. For group analysis, a 2-way ANOVA and Bonferroni post-tests were conducted to identify any interaction in the firing probabilities between the stages of GBL-induced seizure (bursting, continuous SWDs) and firing time intervals (T1 to T4). All statistics were performed in GraphPad Prism 4.

2.3 FUNCTIONAL MAGNETIC RESONANCE IMAGING (fMRI)

Prior to imaging, studies were performed using four rats to characterize the GBL model under isoflurane ranging from 0.75%-2% and ketamine/xylazine (80/10 mg/kg, i.p.). Following GBL injection, EEG suppression was evident using isoflurane in all electrodes and the complete opposite was found under ketamine/xylazine, so it was decided the use of anesthetics was not appropriate for imaging the pharmacological model. Although previous studies in our lab demonstrate the preservation of resting-state networks in the rat under anesthesia (Hutchison, et. al., 2010), this is likely not the case with our chosen pharmacological model to investigate absence seizures. We therefore obtained data collected from Tenney et al., 2003 to analyze functional connectivity between the hippocampus and thalamocortical network.

2.3.1 Acclimation Procedure

Data were provided by Dr. Jeff Tenney from data published in Tenney et al., 2003, which only reported changes in the BOLD signal and not in functional connectivity. The description of the acclimation procedure is therefore derived from Tenney et al., 2003. This study used male Sprague Dawley rats weighing 200-300 grams. Prior to imaging experiments, animals were acclimated to a restrainer to prevent any head and body motion. The restrainer consisted of a multiconcentric Plexiglas head and body holder with built-in radiofrequency dual coil electronics (Insight Neuroimaging Systems, LLC, Orcester, MA, U.S.A.). Rats were anesthetized with medetomidine (Domitor), secured in the restrainer and awakened with Atipamezole (Antiseden), a medetomidine reversal agent. The restraining unit was placed into a black opaque tube to serve as a

'mock scanner' and a tape-recording of an MRI pulse sequence was played for 90 minutes to simulate the sounds within the bore of the magnet. This procedure was repeated for 3-4 days. This acclimation procedure has been shown to significantly reduce body temperature, motion, heart rate and plasma corticosterone levels by the third day of acclimation (King et al., 2005).

2.3.2 fMRI Data Acquisition

All imaging experiments were conducted at the University of Massachusetts Medical School at the Center for Comparative Neuroimaging in Worcester, Massachusetts (Tenney et al., 2003). The description of the acquisition protocol is therefore derived from Tenney et al., 2003. Eight rats were anesthetized with 2 mg ketamine and 0.02 mg medetomidine, fixed with MR-compatible nonmagnetic epidural EEG electrodes, and implanted with an i.p. line for GBL injection. Lidocaine gel was applied to ear canals and the bridge of the nose because these are pressure points in the restrainer. The rats were secured into the restrainer with canines secured over a bite bar and ears positioned inside the head holder. An adjustable surface coil built into the head holder was pressed firmly on the head and locked into place. The body of the rat was placed into the restrainer and the head piece locked into a mounting post on the front of the chassis. A volume coil was slid over the restrainer and locked into position. Antisedan was administered at the time the animal was placed into the head holder and imaging started 30 minutes later.

All images were acquired using a 4.7-T/40-cm (Oxford magnet Technology, Oxford, U.K.) horizontal magnet interfaced to a Paravision console (Bruker Medical

Instruments, Billerica, MA, U.S.A.). High resolution anatomic data were acquired using a fast spin echo (RARE) sequence (TR= 2.5 s; TE= 56 ms; echo train length= 8; field of view= 3 x 3 cm; data matrix= 256 x 256; number of slices= 4; slice thickness= 1.0 mm). Functional images were acquired by a two-segment gradient echo planar imaging (EPI) sequence (TR= 1 s; TE= 25 ms; field of view= 3 x 3 cm; data matrix= 128 x 128; number of slices= 4; slice thickness= 1.0 mm).

Data acquisition followed a specific experimental paradigm (**Figure 7**). EEG data were collected only during breaks in imaging when the scanner was turned off because of the distortions in fMRI images caused by the EEG electrodes. Baseline functional images were collected for 3 minutes, followed by a saline injection and EEG collection for 2 minutes. Functional image acquisition took place for another 2 minutes followed by EEG for 1 minute and then image acquisition for 2 minutes. GBL (200 mg/kg i.p.) was injected, and EEG was recorded for 2 minutes before image acquisition for another 2 minutes. 2 minutes of functional image acquisition was repeated 4 times with EEG wait times of 1 minute, 1 minute, 10 minutes and 30 minutes in between respectively. SWDs were recorded in the EEG, which was reported in the original paper (Tenney et al., 2003), but only the imaging data are included in this thesis.

2.3.3 Data Analysis: fMRI

Brains were extracted from whole brain functional data sets to eliminate non-brain tissue. This was done in FMRIB Software Library (FSL) (The Oxford Centre for Functional MRI of the Brain, Nuffield Department of Clinical Neuroscience, University of Oxford, Oxford) by outlining (masking) the brain in each functional data set – 3
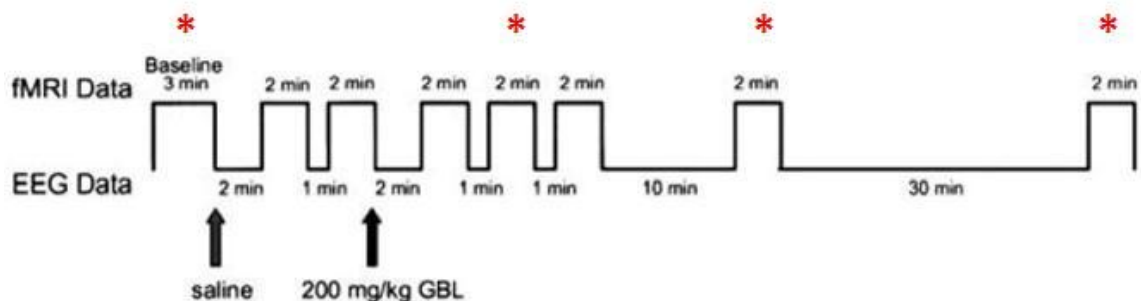
Figure 7. *Specific EEG and functional magnetic resonance imaging experimental paradigm.* EEG data were collected (bottom time periods) during breaks in scanning because of the distortion in the magnet caused by scalp electrodes. The scanner was turned on during time frames indicated at the top of the figure and red asterisks represent time periods (baseline, 5 minutes, 20 minutes, 50 minutes) used for functional connectivity analysis in this thesis. EEG data were not analyzed in this thesis. (adapted from Tenney et. al., 2003).

minute scan for baseline and 2 minute scan for all other time points after injection. All functional connectivity maps were created using Analysis of Functional Neuroimages (AFNI) (National Institute of Mental Health, Bethesda, MD, USA). Data was smoothed (full-width at half maximum = 1 mm) and bandpass filtered between 0.01 and 0.1 Hz and applied to all voxel time courses on a voxel by voxel basis covering the 4 slices of the data sets.

FMRI bold signals from a predefined brain region, called the seed region, was used as a reference to estimate functional connectivity (van den Heuvel & Hulshoff Pol, 2010). Using anatomical scans from the same rat and a rat brain atlas (Paxinos & Watson, 2009) for defining brain structures, seed regions (1 voxel in size – 0.2 x 0.2 mm) were carefully placed in the right thalamus and right dorsal hippocampus of individual rats. The extracted BOLD time course of each seed region was cross-correlated with the BOLD signals of all voxels within the brain to derive corresponding correlational

connectivity maps in baseline and time points (5 min, 20 min, 50 min) after following GBL injection.

3.0 RESULTS

3.1 Local Field Potentials and Behaviour

The stages of seizure development were defined by LFP and behavioural results (**Fig 8A**). Baseline recordings exhibited low amplitude, fast frequency oscillations while rats were immobile and awake. Approximately 4.0 minutes post-GBL injection, the rats experienced intermittent staring spells with simultaneous bursts of SWDs (**Fig. 8B**) of larger amplitude and rhythmic oscillations in all recording electrodes. At 8.8 minutes post-injection, rats became completely immobile and experienced a vacant stare along with abrupt facial and vibrissae twitching. At the same time, EEG displayed continuous SWDs (**Fig. 8B**) in all recordings electrodes. After an average of 52.3 minutes post-injection, the rats experienced either an abrupt head shake or body jerk and continued to explore the Plexiglas cage, eat and drink. At the time of the abrupt head shake, EEG returned to baseline with the disappearance of SWDs.

Power spectra express the amplitude of the neural signal in the brain region as a function of frequency. The peak frequency was analyzed from the power spectra of the LFPs in all rats during baseline, bursting SWDs and continuous SWDs (**Fig. 9**). No significant peaks were identified during baseline recordings, however peaks were identified post-GBL injection. The range of peak frequencies among all brain regions during the bursting SWDs was 4.98-5.24 Hz, whereas the range of peak frequencies

during the continuous stage decreased to 2.64-3.59 Hz (**Table 1**). Nonparametric Mann Whitney U tests revealed a significant decrease in peak frequency from the bursting to the continuous stage of SWDs in the parietal cortex ($U = 2$, $p < 0.0001$), the hippocampus ($U = 3.5$, $p < 0.01$), the frontal cortex ($U = 3$, $p < 0.01$), the ventrolateral thalamus ($U = 0.5$, $p < 0.0001$), and the visual cortex ($U = 1$, $p < 0.0001$). Following GBL injection, there was a general increase in EEG power in the 2-6.5 Hz frequency range at all electrodes (**Fig. 10**), as compared to the EEG during immobility before injection. Non-parametric Kruskal-Wallis tests revealed a significant increase in 2-6.5 Hz EEG power in the parietal cortex ($KW = 9.905$, $p < 0.005$), the hippocampus ($KW = 7.955$, $p < 0.1$), the frontal cortex ($KW = 14.74$, $p < 0.001$), the ventrolateral thalamus ($KW = 10.99$, $p < 0.01$) and the visual cortex ($KW = 7.845$, $p < 0.05$). In the parietal cortex, Dunn's Multiple Comparison test revealed a significant increase in power between baseline and the bursting stage ($p < 0.05$) and between baseline and the continuous stage ($p < 0.05$). There was no significant change in power between the bursting and continuous stage ($p > 0.05$). In the hippocampus, Dunn's Multiple Comparison test revealed a significant increase only between baseline and the bursting stage ($p < 0.05$). In the frontal cortex, Dunn's Multiple Comparison test revealed a significant increase in power between baseline and bursting stage ($p < 0.001$) and between baseline and the continuous stage ($p < 0.05$). In the ventrolateral thalamus and the visual cortex, Dunn's Multiple Comparison test revealed a significant increase in power only between baseline and the bursting stage ($p < 0.01$ and $p < 0.05$ respectively). No significant change in power was revealed between the bursting and continuous stages ($p > 0.05$).
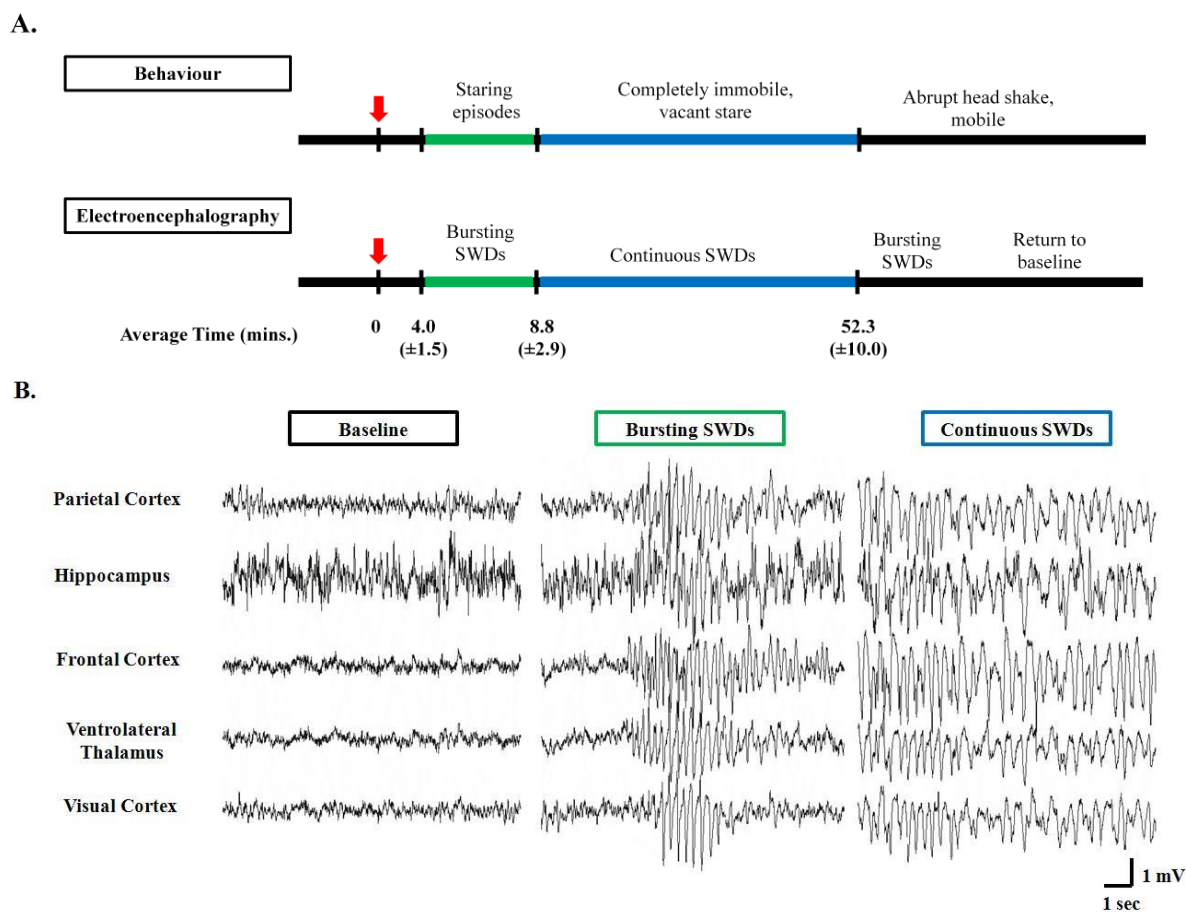
Figure 8. *Behaviour and local field potentials in the GBL rat model of absence seizures.* The head cap was connected to the EEG recording system and baseline was recorded once the rats were completely immobile and awake. Rats were injected with 200 mg/kg GBL (i.p.) and LFPs were recorded for 2 hours following injection. **(A)** Stages of seizure development were characterized based on behavioural and EEG findings following GBL injection. Time (minutes) is presented as mean and standard deviation. **(B)** Example of electrographic recordings of a single rat in all five recording electrodes during the identified stages. EEG was filtered between 0.3-70 Hz and sampled at 200 Hz. (SWDs: spike-and-wave discharges)
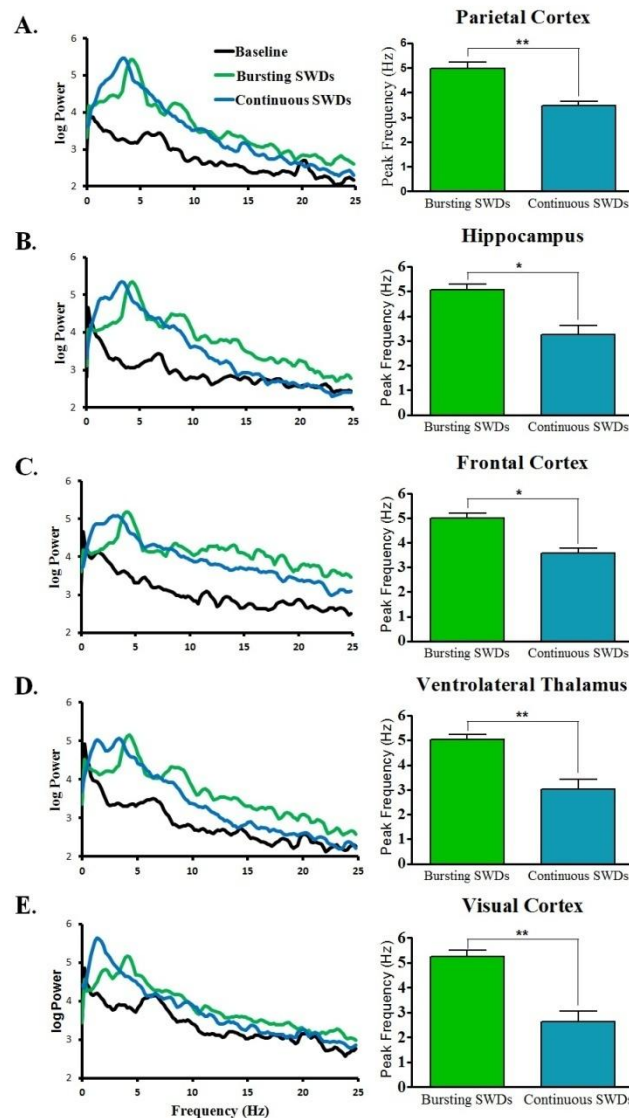
Figure 9. *Power spectra and peak frequency in brain regions following GBL injection.* The left column displays example power spectra of a representative rat in different brain regions. The right column displays the changes in peak frequency of the bursting and continuous stages of spike-and-wave discharges (SWDs) following i.p. injection of GBL in all rats (n=8) in the parietal cortex **(A)**, hippocampal CA1 region **(B)**, frontal cortex **(C)**, ventrolateral thalamus **(D)** and visual cortex **(E)**. Peak frequencies during each stage were identified in the power spectra generated by a Fast Fourier Transform. No peaks were identified in any of the baseline recordings, however peaks were identified during the presence of SWDs. Mann-Whitney U tests were conducted on each brain region to determine any differences in peak frequency. A significant decrease was revealed from the bursting to the continuous stage of SWDs. The range of peak frequencies in all brain regions during the bursts of SWDs was 4.98-5.24 Hz. The range of peak frequencies in all brain regions during the continuous stage of SWDs was 2.64-3.59 Hz. Results expressed as mean and SEM (*P<0.01, **P<0.001).

Table 1. Mean and standard deviation of the frequency of peak power (in Hz) in different brain regions during the bursting and continuous stages of absence seizure induced by GBL

Brain Region	Bursting SWDs		Continuous SWDs	
	Average	Range	Average	Range
Parietal Cortex	4.98 (0.73)	4.10-6.06	3.47 (0.52)	2.93-4.30
Hippocampus	5.08 (0.64)	4.28-6.06	3.23 (1.0)	2.93-4.30
Frontal Cortex	5.01 (0.57)	4.30-6.06	3.59 (0.58)	3.13-4.69
Ventrolateral Thalamus	5.05 (0.54)	4.30-6.06	3.03 (1.0)	1.76-4.30
Visual Cortex	5.24 (0.69)	4.10-6.25	2.64 (1.1)	1.17-4.30

(n=8) Values in parenthesis represent standard deviation.
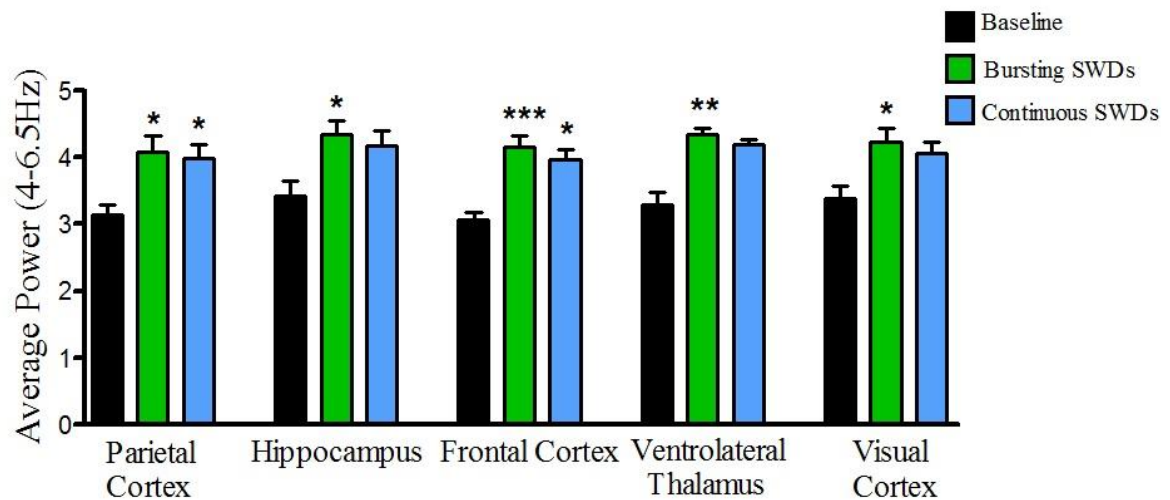
Figure 10. *Local field potential power changes following GBL injection.* EEG power was averaged in each rat (n=8) between 2-6.5 Hz to determine changes in power throughout seizure stages. Kruskal-Wallis tests were conducted on each brain region and revealed a significant increase (P-values<0.05) in power from baseline following GBL injection. Dunn's Multiple Comparison tests showed no significant change in power between the bursting and continuous stage of spike-and-wave discharges (SWDs) in all brain regions, but did reveal a significant increase when compared to baseline. Results are expressed as mean and SEM (*P<0.05, **P<0.01, ***P<0.001).

Coherence of the LFPs between all pairs of recording electrodes, for a total of 10 pairs, was investigated. The general trend among all pairs was an increase in coherence at the 2-9 Hz range (**Fig. 11**) following GBL injection, however the increase was found to be statistically significant in only five pairs (**Fig. 11A**). The pairs that showed statistically significant increases in coherence, as analyzed by non-parametric Kruskal-Wallis test, were: (1) parietal cortex-hippocampus, KW = 8.765, $p < 0.05$; (2) parietal cortex-ventrolateral thalamus, KW = 6.914, $p < 0.05$; (3) hippocampus-frontal cortex, KW = 7.035, $p < 0.05$; (4) hippocampus-ventrolateral thalamus, KW = 7.955, $p < 0.05$; and (5) hippocampus-visual cortex, KW = 3, $p < 0.05$. Each pair exhibited enhanced synchronization in a similar manner, indicated by increase in coherence, or positive slope, from baseline to bursting SWD stage (**Fig. 11A**). Each pair exhibited a decrease in coherence from the bursting to the continuous SWD stage, but the coherence remained above baseline values throughout all SWD stages. All pairs that included the hippocampus exhibited increases in coherence during the seizure stages. Dunn's Multiple Comparison tests showed no significant difference between coherence in baseline and continuous SWDs, but did show a significant increase in coherence from baseline to bursting SWDs for the parietal cortex and hippocampus pair ($p < 0.05$), the parietal cortex and ventrolateral thalamus pair ($p < 0.05$) and the hippocampus and visual cortex pair ($p < 0.05$). There were no significant changes (**Fig. 11B**) in LFP coherence of the remaining pairs from different brain regions ($p > 0.05$).

3.2 Neuronal Unit Recordings

The thalamic and hippocampal LFP exhibited changes in peak frequencies following GBL injection as expected from the previous experiments. A peak frequency was identified between 4-6 Hz during bursting SWDs followed by a decrease to 2-4 Hz during continuous SWDs (**Fig. 12**). No prominent peaks were identified at higher frequencies in the hippocampal power spectra, however there was an increase in power between 50-100 Hz in the thalamic signal following GBL injection (**Fig. 12B**). This increase in 50-100 Hz thalamic power was not observed in the previous EEG analysis (**Fig. 9-10**) because of input filter cut off at 70 Hz.

Overall there was a decrease in the average unit firing of hippocampal neurons following GBL injection and this was considerably reduced during continuous SWDs (consistent in 4 of 6 rats), and the most frequent firing was present within 250 msec prior to (consistent in 5 of 6 rats) thalamic SWD detection (**Table 2**). A 2-way ANOVA identified a significant interaction between stage of GBL-induced seizure (baseline, bursting SWDs, continuous SWDs) and probability of hippocampal neuronal firing (T1, T2, T3, T4) in relation to thalamic SWDs ($F(6, 60) = 5.288$, $p = 0.0002$) (**Fig. 13**). Bonferroni post-tests identified a significant increase in hippocampal neuronal firing in T2 from both baseline ($t = 4.336$, $p < 0.001$) and bursting SWDs ($t = 3.667$, $p < 0.01$) to continuous SWDs. There was also a significant decrease in hippocampal neuronal firing in T1 from baseline to continuous SWDs ($t = 2.708$, $p < 0.05$).
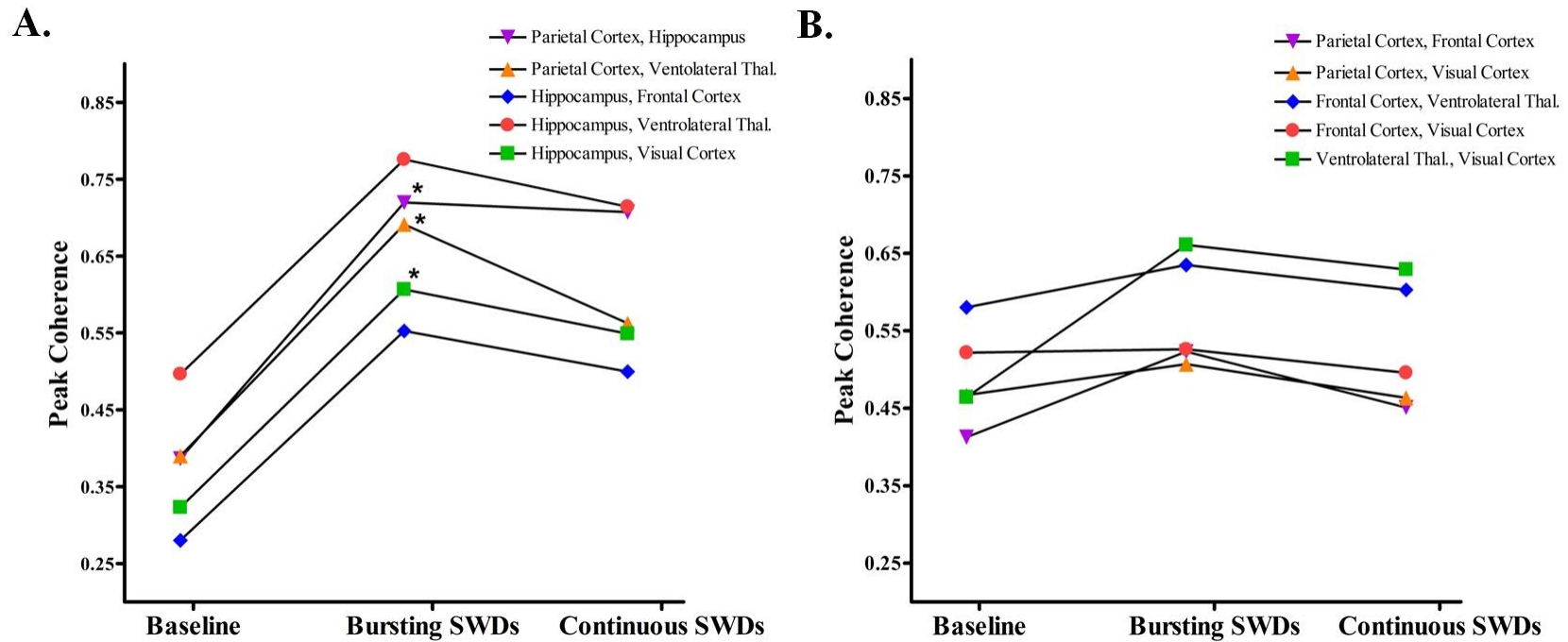
Figure 11. *Changes in coherence between brain regions following GBL injection.* Highest coherence values were identified between 2-9 Hz after comparing all possible pairs of recording electrodes using coherence spectral analysis (n=8). **(A)** Kruskal-Wallis tests revealed a significant increase (P-values<0.05) in coherence between pairs of recording electrodes. Dunn's Multiple Comparison tests showed no significant difference between coherence in baseline and continuous spike-and-wave discharges (SWDs), but did show a significant increase in coherence from baseline to bursts of SWDs in three of the five significant pairs (*P<0.05). **(B)** Kruskal-Wallis tests revealed no change in coherence between pairs of recording electrodes. Values are expressed as mean (SEM error bars are presented in **Appendix A**).

In a representative rat, there was a decrease in firing following GBL injection. The probability of firing in T1, T3 and T4 continued to decrease from baseline, however the frequency of firing in T2 increased from baseline. Although baseline firing appeared uniform (**Fig. 14**), nonparametric Kruskal-Wallis tests and Dunn's Multiple Comparison post-tests demonstrated a significant difference between T1 and T4 (KW = 12.76, p < 0.01). Unit firing in T2 and T3 was uniform throughout baseline, however as the relative firing in T2 increased and the relative firing in T3 decreased, there was a significant difference between these time intervals (KW = 10.77, p < 0.01) in bursting SWDs (**Fig. 15**). As the relative unit firing increased in T2, all other time intervals exhibited a significant difference compared to T2 during continuous SWDs (**Fig. 16**). The relative cell firing in T1 (KW = 17.96, p < 0.05) and T4 (KW = 9.997, p < 0.05) significantly decreased from the bursting and continuous stage of SWDs. The relative cell firing in T1 (KW = 17.96, p < 0.001), T3 (KW = 15.52, p < 0.001) and T4 (KW = 9.997, p < 0.05) significantly decreased from baseline to the continuous SWDs.

Figure 12. *Power spectra in the hippocampus (recorded at CA1 cell layer) and ventrolateral thalamus following GBL injection of neuronal unit recordings.* Example average power spectra (duration of signal analyzed is 3 minutes and each second yields a power spectrum), generated by a Fast Fourier Transform, are of a representative rat in the hippocampus (**A**) and the thalamus (**B**). The inset of each power spectrum (above) exhibit the characteristic peak frequency of 4-6 Hz during bursting spike-and-wave discharges (SWDs) and 2-4 Hz during continuous SWDs.

Table 2. Number of CA1 neuronal firing counts detected by thalamic spike-and-wave discharges (SWDs) in each subject during bursting and continuous stages of SWDs induced by GBL

	T1	T2	T3	T4	Total
Rat A					
Baseline	94	79	51	29	**253**
Bursting SWDs	56	124	24	30	**234**
Continuous SWDs	3	108	1	3	**115**
Total	**153**	**311**	**76**	**62**	
Rat B					
Baseline	134	106	89	47	**370**
Bursting SWDs	978	913	425	279	**2595**
Continuous SWDs	4	71	3	7	**85**
Total	**1116**	**1090**	**517**	**333**	
Rat C					
Baseline	398	560	158	84	**1200**
Bursting SWDs	89	107	100	19	**315**
Continuous SWDs	366	324	88	28	**806**
Total	**853**	**991**	**346**	**131**	
Rat D					
Baseline	255	383	150	1000	**888**
Bursting SWDs	5	10	17	10	**42**
Continuous SWDs	3	87	83	5	**178**
Total	**263**	**480**	**250**	**115**	
Rat E					
Baseline	986	1532	1446	327	**4291**
Bursting SWDs	505	1002	271	215	**1993**
Continuous SWDs	122	389	80	70	**661**
Total	**1613**	**2923**	**1797**	**612**	
Rat F					
Baseline	458	412	233	110	**1213**
Bursting SWDs	102	166	62	19	**349**
Continuous SWDs	10	70	10	14	**114**
Total	**580**	**648**	**305**	**143**	

T1: -500 ms to -250 ms, **T2** : -250 ms to 0, **T3** : 0 (event detection) to 250 ms, **T4** : 250 ms to 500 ms
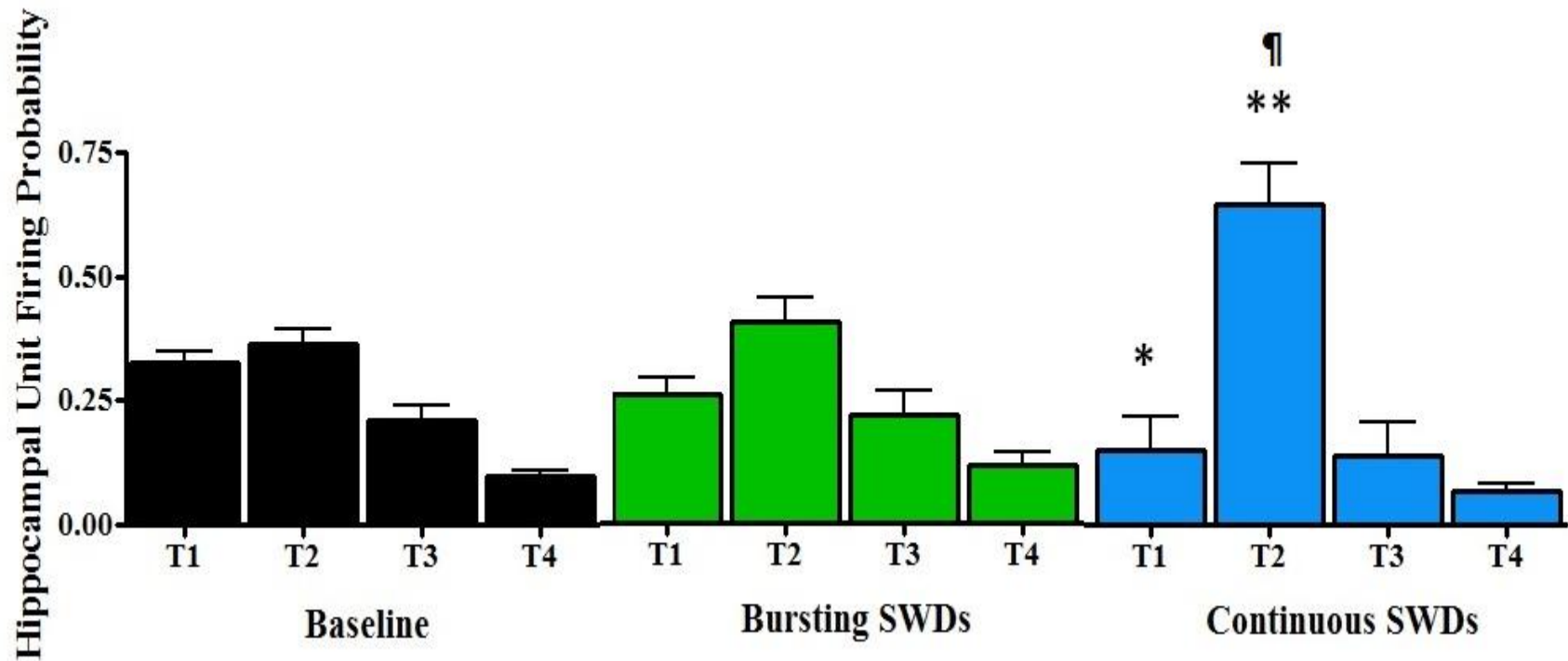
Figure 13. *Hippocampal neuronal firing in relation to GBL-induced thalamic SWDs.* A threshold was set to detect the negative peak of the thalamic spike-and-wave discharges (SWDs). Event detection was used to identify hippocampal neuronal unit firing 500 to 250 msec prior (T1), 250 msec to event detection (T2), 250 msec after (T3) and 250 to 500 msec after event detection. A 2-way ANOVA and Bonferroni post-tests identified a significant interaction between time intervals T1-T4 and stage of GBL-induced SWDs ($F_{(6, 60)}$ = 5.288, p = 0.0002). Results are expressed as average (n=8) probability of hippocampal unit firing. (*P<0.05 and **P<0.001 compared to baseline, ¶P<0.01 compared to bursting SWDs)
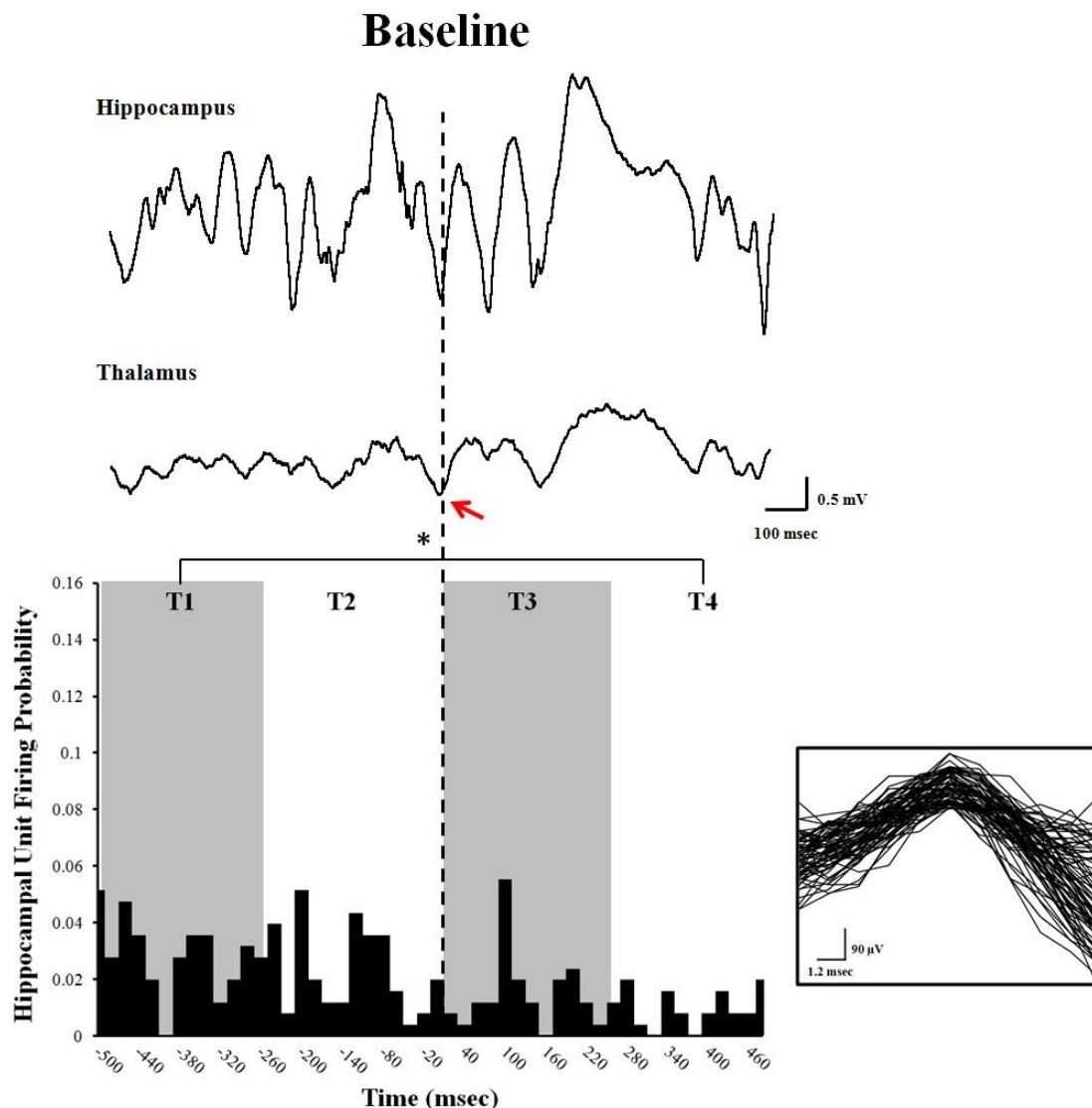
Figure 14. *Hippocampal neuronal firing in relation to thalamic local field potentials in baseline.* A threshold was set to detect the negative peak of the thalamic EEG (event detection indicated by red arrow). Event detection (time 0 indicated by vertical dashed line) was used to identify hippocampal neuronal unit firing 500 msec before and 500 msec after detection. Examples are from a single representative rat. Hippocampal and thalamic LFP traces were averaged after 40 event detections (upper traces) and hippocampal pyramidal cell firing count in relation to event detection is represented in the time histogram. A Kruskal-Wallis test identified no significant differences in relative neuronal unit firing, except between T1 and T4. The neuronal unit overlay to the right displays all 253 sweeps that contributed to the time histogram. (T1: -500 ms to -250 ms, T2 : -250 ms to 0, T3 : 0 to 250 ms, T4 : 250 ms to 500 ms, *P< 0.01)
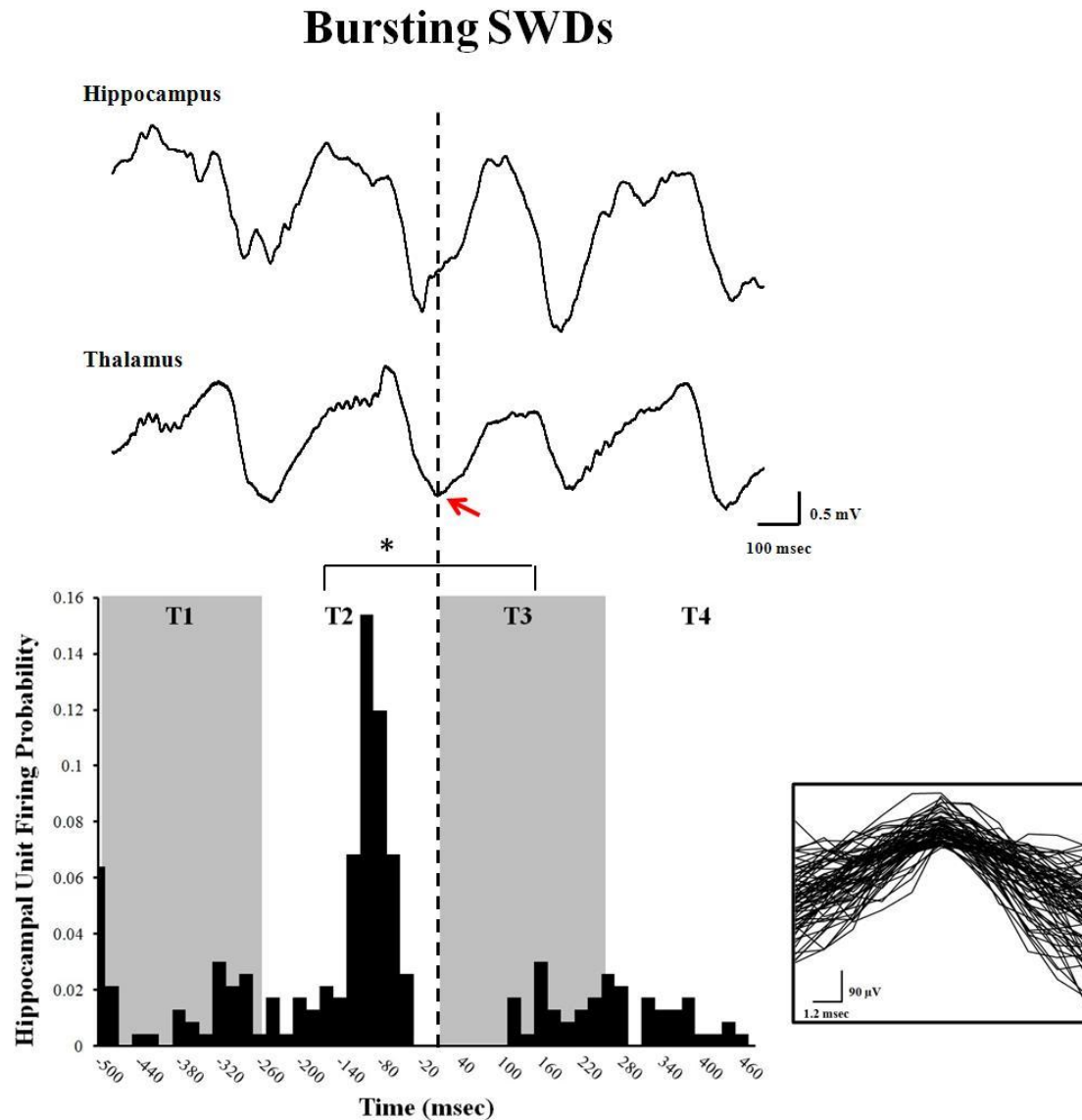
Bursting SWDs

Figure 15. *Hippocampal neuronal firing in relation to the negative peak of thalamic SWDs in bursting SWDs.* A threshold was set to detect the negative peak (red arrow) of the thalamic SWD (spike-and-wave discharge). Event detection (time 0 indicated by vertical dashed line) was used to identify hippocampal neuronal unit firing 500 msec before and 500 msec after detection. Examples are from a single representative rat. Hippocampal and thalamic EEG traces were averaged after 40 event detections (upper traces) and hippocampal neuronal firing count in relation to event detection is represented in the time histogram. A Kruskal-Wallis test identified no significant differences in relative neuronal unit firing across the 1000 msec, except between T2 and T3. The neuronal unit overlay to the right displays all 234 sweeps that contributed to the time histogram. (T1: -500 ms to -250 ms, T2 : -250 ms to 0, T3 : 0 to 250 ms, T4 : 250 ms to 500 ms, *P< 0.01)
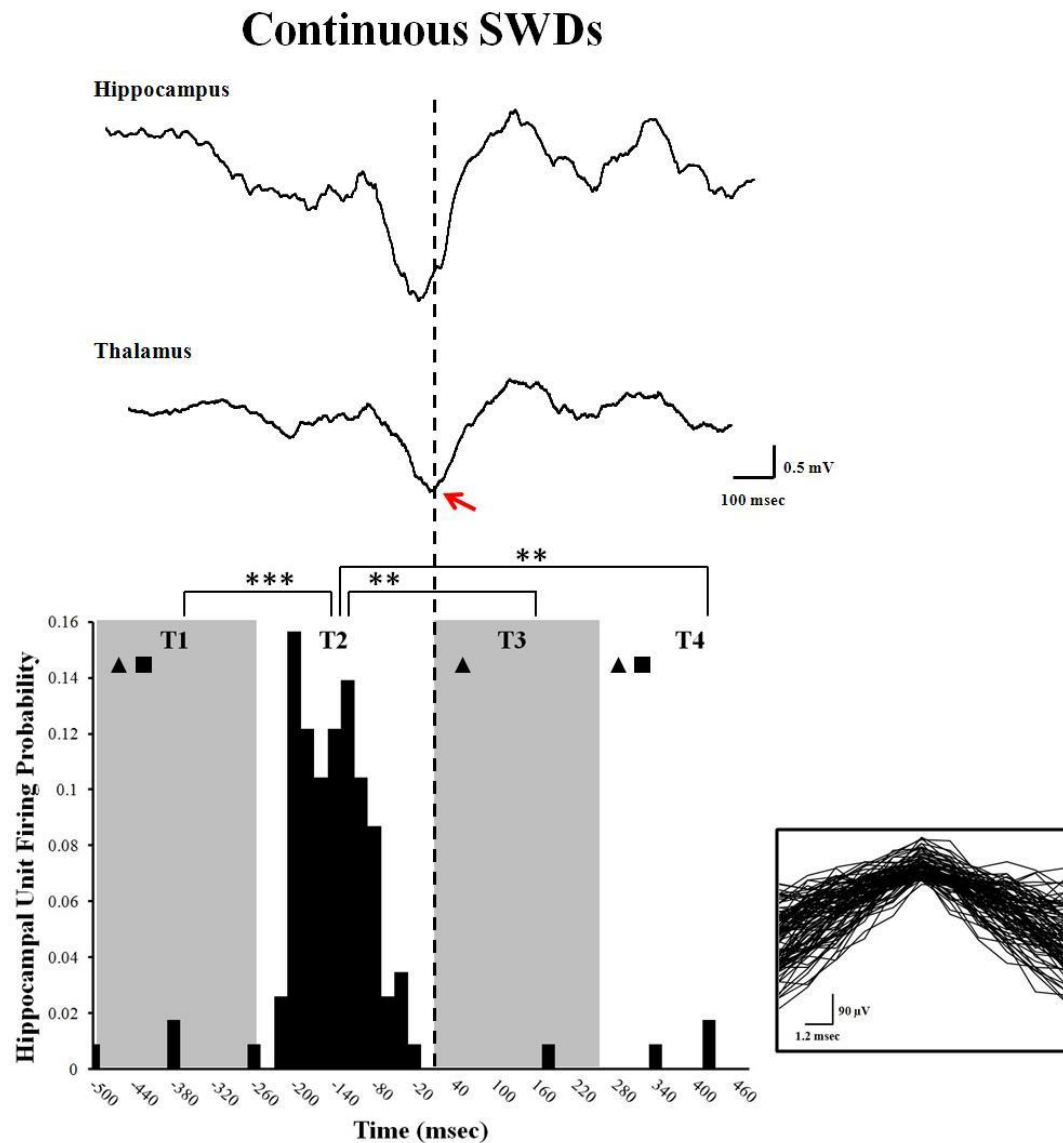
Figure 16. *Hippocampal neuronal firing in relation to the negative peak of thalamic SWDs in continuous SWDs.* A threshold was set to detect the negative peak (red arrow) of the thalamic SWD (spike-and-wave discharge). Event detection (time 0 indicated by vertical dashed line) was used to identify hippocampal neuronal unit firing 500 msec before and 500 msec after detection. Examples are from a single representative rat. Hippocampal and thalamic EEG traces were averaged after 40 event detections (upper traces) and hippocampal neuronal firing count in relation to event detection is represented in the time histogram. Kruskal-Wallis and Dunn's Multiple Comparison tests showed significant differences (P-values<0.05) in relative neuronal unit firing between T1 and T2, T2 and T3, and T2 and T4. Kruskal-Wallis and Dunn's Multiple Comparison tests identified significant decreases in relative neuronal unit firing from baseline (solid triangle) and from bursting SWDs (solid square). The neuronal unit overlay to the right displays all 115 sweeps that contributed to the time histogram. (T1: -500 ms to -250 ms, T2 : -250 ms to 0, T3 : 0 to 250 ms, T4 : 250 ms to 500 ms, **P< 0.01, ***P<0.001)

3.3 Functional Connectivity

The functional connectivity of the thalamus and hippocampus with the rest of the brain during the GBL-induced seizure was investigated using a seed-based approach (Hutchison et. al., 2010; 2011). Functional connectivity maps of a representative rat are shown in **Figure 17**, in which a thalamic seed was placed as close to the ventrolateral thalamus (right hemisphere) as possible. Baseline maps revealed bilateral activation in the thalamus and parts of the neocortex. Seed-region analysis revealed synchronized BOLD signal after 5 minutes between the seed region and the hippocampus, the caudate putamen and the widespread regions of the neocortex. The seed region was highly synchronized with the primary somatosensory cortex (barrel cortex). Functional connectivity with the seed region decreased after 20 minutes and became more localized to regions of the thalamus and dispersed within the neocortex. After 50 minutes, analysis revealed widespread synchronization of the BOLD signal between the thalamus and the neocortex. Overall, the thalamus exhibited increased functional connectivity with different regions of the brain following GBL injection.

Functional connectivity maps of the same rat are shown in **Figure 18**, in which a hippocampal seed was placed as close to the CA1 region (right hemisphere) as possible. Baseline maps revealed bilateral activation in parts of the neocortex and the hippocampus. With the progression of time, the seed region sustained synchronization with the thalamus, neocortex and the caudate putamen. Overall, the hippocampus exhibited the highest connectivity with the cortex as represented in the connectivity maps.
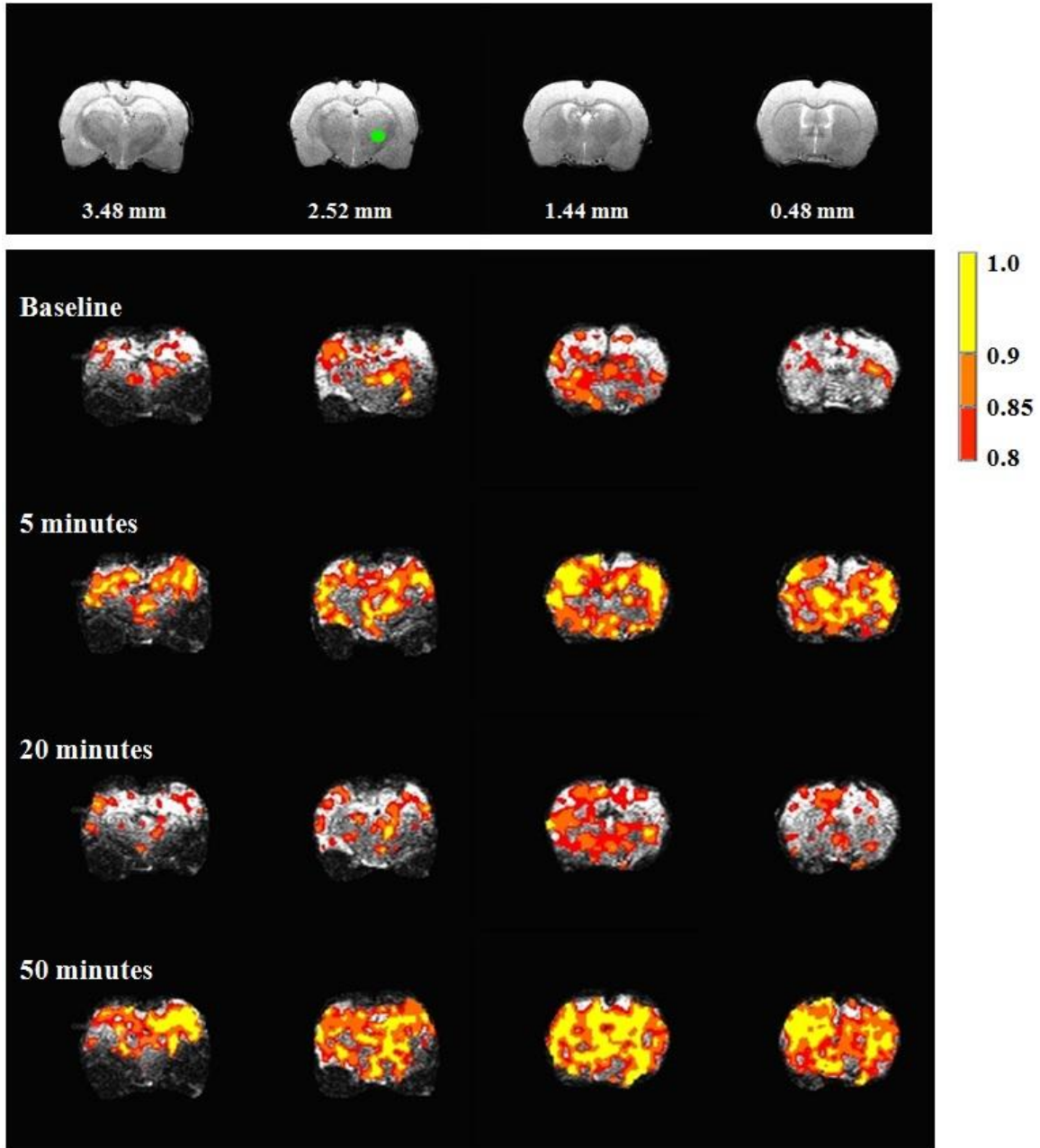
Figure 17. *Pharmacological resting-state functional connectivity of GBL-induced absence seizures in a representative rat using thalamic seed-region analysis.* Correlation coefficient maps were calculated by correlating the time course of all voxels with the average time course of the seed placed in the thalamus (green circle). Coronal anatomical images are displayed in the top panel with the distance of each slice posterior to bregma. Coronal functional images are displayed in the bottom panel with 0 minutes used as time of GBL injection. The threshold used for all images was a correlation coefficient of 0.8 as indicated by the colour bar.
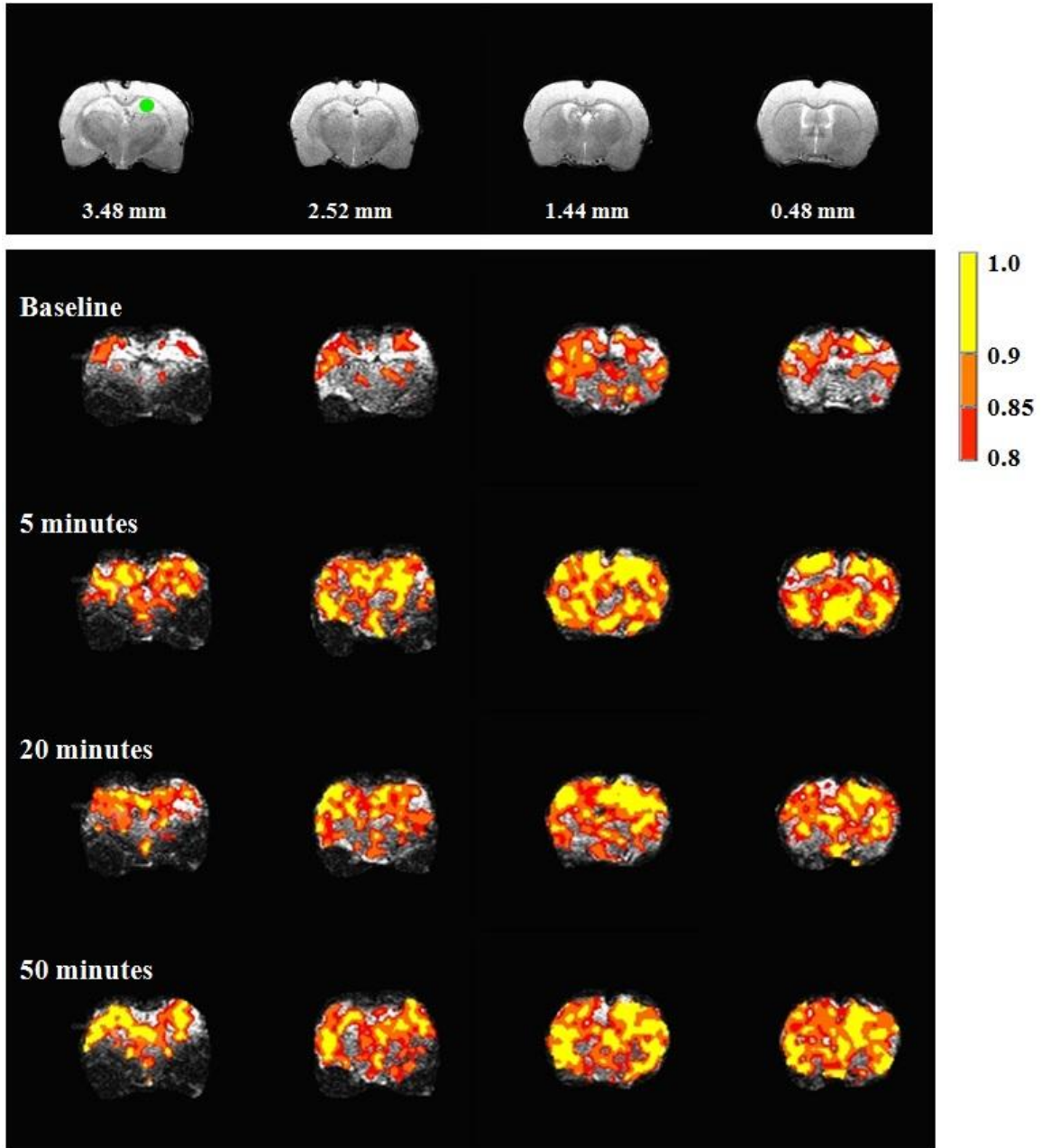
Figure 18. *Pharmacological resting-state functional connectivity of GBL-induced absence seizures in a representative rat using hippocampal seed-region analysis.* Correlation coefficient maps were calculated by correlating the time course of all voxels with the average time course of the seed placed in the hippocampus (green circle). Coronal anatomical images are displayed in the top panel with the distance of each slice posterior to bregma. Coronal functional images are displayed in the bottom panel with 0 minutes used as time of GBL injection. The threshold used for all images was a correlation coefficient of 0.8 as indicated by the colour bar.

4.0 DISCUSSION

The primary goal of this thesis was to investigate whether or not the hippocampus becomes entrained in SWDs following thalamocortical activation using a pharmacological rat model of absence seizures. Although none of the major theories include a role for the hippocampus, our motivation was to understand how and why there is great variation among patients with absence epilepsy that present with severe cognitive impairment and memory loss (Caplan et al., 2008). We investigated hippocampal activation using local field potentials, coherence analysis, neuronal unit firing recordings and functional magnetic resonance imaging. We hypothesized that the hippocampus may become entrained in SWDs following thalamocortical activation.

4.1 Coherence of Hippocampal, Thalamic and Neocortical Local Field Potentials

The local field potential and behavioural results following GBL injection corroborate early findings since the discovery of the GBL rat model of absence seizures. Four to 6 Hz SWDs, behavioural arrest and facial twitching were observed in these experiments and are characteristic of several absence seizure models. Following GBL injection, the first observed change in EEG was a brief period of synchronous bursts of SWDs in all recorded regions of the brain, including the hippocampus. Shortly after, there was a progression into a continuous stage of hypersynchronization associated with complete immobility, blank stares and some facial and vibrissae twitching. One of the only studies to report this continuous stage in the GBL model also looked at similar brain areas (Banerjee et al., 1993). Using GHB autoradiography, this study demonstrated that increases in GHB binding in the reticular thalamic nucleus peaked at the onset of SWDs

and gradually declined throughout the duration of the seizure. This supports the critical role of this thalamic nucleus in the generation of GHB-induced SWDs. There was also an increase in GHB binding in the neocortex, which explains the presence of SWDs in the frontal cortex, visual cortex, parietal cortex and the thalamus in this model. Interestingly, the same study found that the hippocampus has the highest density of GHB binding sites, but failed to record any SWDs. This is contradictory to our findings perhaps because they recorded from the CA3 region, whereas we recorded SWDs in the hippocampal CA1 region.

There are inconsistencies among animal models of absence seizures surrounding the primary thalamic nuclei that contribute to the generation of SWDs, however there is some agreement that it is either the ventrolateral (VL) or ventroposteromedial (VPM) nucleus. The VPM is a good candidate because there are clusters of cell bodies in layer IV of the rat somatosensory cortex that receive somatotopically organized projections from VPM (Agmon & Connors, 1991). These cell bodies are considered to be the functional units that receive information from single vibrissae. Although we did not record from the VPM, its involvement would explain the sudden twitching of the vibrissae and the facial muscles of the rat during the seizure. The reason we chose to record from VL is because projections from VL terminate in the superficial layers of the rat motor cortex (Herkenham, 1980), where there are high densities of GHB binding sites (Banerjee et al., 1993). VL in the rat is considered the primary relay motor nucleus which receives afferents from several extrathalamic motor regions including the basal ganglia (Lukhanina, 1994). Based on the motor arrest of the rat during GBL-induced absence seizures, VL is expected to play a role in SWDs and indeed, SWDs were present in both

VL and the parietal cortex (**Fig 8B**.), to which VL projects. It is not likely however, that a single thalamic nucleus acts alone to generate SWDs. A more plausible explanation would be that several relay nuclei participate in SWDs simultaneously. The reticular thalamic nucleus has reciprocal projections with all relay nuclei, so VL and VPM may both be active during the generation of SWDs. There are other thalamic nuclei that may also be potential candidates, which is discussed below.

As demonstrated in Figure 9, all recorded brain regions displayed a peak frequency between 4-6 Hz during bursting SWDs and this peak frequency decreased during continuous SWDs to between 2.5-4 Hz. The GBL-induced bursting stage of SWDs resembles that of the common human absence seizure lasting no longer than 20 seconds (International League Against Epilepsy, 1981), and the continuous stage and reduction in peak frequency is rare but also characteristic in humans and is referred to as absence status epilepticus (Baykan et. al., 2002). This stage in the rat model may also be a result of the drug itself and the fact that GBL can be taken up from the blood following injection. GBL is lipid-soluble, so lean muscle can sequester a large portion, which may slow down its metabolism and prolong its transport to the brain (Roth & Giarman, 1966). Regardless, it is not surprising that peak frequencies changed concurrently among all recorded regions during a generalized seizure. Additionally, it is not surprising that the respective power dominated across the frequency spectrum in Figure 10.

By definition, the term *generalized* seizure implies that many parts of the brain become involved almost synchronously during a generalized seizure. However, it is becoming more and more apparent that there may be selective thalamocortical involvement, and that some brain structures participate more than others and some not at

all (Holmes et al., 2004). We therefore analyzed coherence of LFPs among implanted depth electrodes. If generalized seizures were truly generalized, we would expect to find coherence among all regions to a similar magnitude. This was not the case however, as evident in Figure 11. The results indicate that coherence was not uniform among different pairs of brain regions. Out of the 10 pairs of regions analyzed, only 5 demonstrated significant changes in coherence with different stages of SWDs. The synchronization between the VL and parietal cortex is representative of the thalamocortical circuit and its involvement is supported by direct projections from VL into the parietal cortex (motor cortex) of the rat brain. The novel finding is that all remaining pairs with significant changes in coherence included the hippocampus. During bursting SWDs, the CA1 region of the hippocampus exhibited enhanced neural coherence with the parietal, frontal, and visual cortex and the thalamus.

Local field potentials reflect synchronous postsynaptic potentials in a local population of neurons (Leung, 2010). The increased power at 4-6 Hz in the LFPs at each brain site (thalamus, neocortex or hippocampus) is indicative of increased number of participating neurons and increased synchronization among neurons. However, coherence of field potentials between two distant brain areas suggests common connections between the two regions (e.g., hippocampus and thalamus). The latter could be interpreted as an increase in direct connection between the thalamus and the hippocampus. However, the involvement of multi-synaptic connections between the thalamus and the hippocampus is possible, in particular in relation to synchrony of a relatively slow event of 4-6 Hz, e.g., delays of 20 ms will represent only 10% of the period of a 5-Hz rhythm, and many synapses can be involved with a 20 ms delay. In addition, if a third brain area projects

common inputs to both regions (hippocampus and thalamus), the signals in the two regions can be coherent as well, without having direct or indirect connections with each other. Also important is that hippocampal SWDs were not independent of cortical and thalamic SWDs but were concomitant, which suggests that they are being driven by the same pacemaker, whether it be the cortex or the thalamus. The identification of SWDs in the hippocampus and its coherence with the cortex and the thalamus suggest an important relationship between hippocampal activity and absence seizures. To elucidate the nature of this relationship we assessed hippocampal neuronal activity during GBL-induced absence seizures by recording from the CA1 pyramidal cell layer.

4.2 Time-locked Hippocampal Neuronal Firing

In our next experiments, we implanted depth electrodes into the CA1 pyramidal cell layer of the hippocampus and the thalamus with the goal of characterizing the temporal relationship of hippocampal neuronal firing in relation to SWDs. We predicted an increase in CA1 neuronal unit firing after GBL injection. After setting a threshold to detect the negative peak of thalamic SWDs, the most frequent hippocampal firing was consistently found within 250 msec preceding the thalamic SWD. Although there were no evident peaks at higher frequencies in the power spectrum, Figure 12 demonstrates an increase in 50-100 Hz power in the thalamus, which may likely correspond to the high frequency oscillation evident on the thalamic wave 250 msec preceding detection in Figure 15. The time-locked firing of hippocampal unit activity is evidence that the hippocampus influences thalamocortical SWDs, perhaps by driving activation of specific thalamic nuclei either directly or via the reticular thalamic nucleus (Cavdar et al., 2008).

The hippocampus is perhaps involved in maintenance and regulating SWDs. While the hippocampus influences thalamocortical SWDs by maintaining its time-locked firing ~250 msec prior to the thalamic SWD, it is also apparent that after prolonged exposure of the brain to hypersynchronous activation, the hippocampus begins to progressively decrease in activity. Important to keep in mind is that the hippocampus is active during both bursting and continuous SWDs, which are both reminiscent in human absence seizures and that this activity is time-locked with thalamic SWDs.

4.3 Functional Connectivity between the Hippocampus and Thalamocortical Network

We have thus far demonstrated time-locked firing of the hippocampus during SWDs and synchronization of hippocampal LFPs with those in the thalamus and neocortex. However, the spatial resolution of EEG is constrained to tens or hundreds of neurons, placing a lower limit on the effective spatial resolution in relation to the rest of the brain (Keogh & Cordes, 2007; Mirsattari et. al., 2007). As an additional measure we used pharmacological resting-state fMRI to study the functional connectivity between the hippocampus and the rest of the brain, including the thalamus and neocortex.

The functional connectivity of the brain can be measured by the temporal relationship of the blood-oxygen-level dependent (BOLD) signals (Ogawa et al., 1990) in two regions of the brain. Functional connectivity represents a novel approach to fMRI which allows the investigation of active regions even when they are anatomically distant (Aertsen et al., 1989). Areas of the brain that exhibit BOLD signal fluctuations correlated in time are assumed to be functionally connected and therefore demonstrate a level of co-activation.

The BOLD time-course correlation analysis can produce functional connectivity maps showing which areas are connected with the given seed region and to what extent (Rosazza & Minati, 2011). The seed voxel or region is identified as an area of interest in the brain found or believed to be active during a specific task, or in our studies, believed to be involved in spike-and-wave discharges. Therefore our seed regions are the thalamus and hippocampus.

These data were analyzed from an experiment conducted in 2002 and published in 2003 by Dr. Jeff Tenney. The difference with their analysis was that they used neocortical and thalamic regions of interest for the purpose of assessing changes in BOLD signal intensity solely within those regions. They predominantly found positive BOLD changes in the thalamus with mixed positive and negative BOLD changes in the neocortex and did not report any changes in the hippocampus. However, changes in BOLD signals in one region tells us nothing about how it changes in relation to other regions of the brain, which is why we studied functional connectivity patterns using temporal correlation of the BOLD signal fluctuations.

Based on the previous experiments, we predicted that the hippocampus would exhibit increased BOLD signal and become functionally connected with the thalamus and neocortex following GBL injection. We found that the hippocampus becomes functionally connected with the neocortex and the thalamus during bursting SWDs (5 minutes after injection) and this connectivity endures during the continuous SWD stage (20 and 50 minutes) as presented in Figure 18. The fMRI connectivity maps using a seed in the ventrolateral nucleus confirm the strong connectivity with the hippocampus. Figure 17 demonstrates functional connectivity of the hippocampus and the thalamus

during bursting SWDs (5 minutes after injection) and then again in the late stage of continuous SWDs (50 minutes after injection). Interestingly, correlations between regions are relatively high following GBL injection, evident in the fact that the threshold used to clearly visualize correlational changes was set to 0.8. These functional connectivity maps complement the coherence analysis in our LFP experiments by providing higher spatial resolution of the entire brain during the development of SWDs. Typically, fMRI protocols have a low temporal resolution and our data was acquired by collecting volumes of data every 2.5 seconds (TR = 2.5). This demonstrates why it was important to combine EEG data with good temporal resolution and fMRI data with good spatial resolution. Using EEG, we are able to record individual SWDs, while using fMRI, we can follow the spread of hypersynchronous activity as a result of SWDs throughout the rest of the brain. These experiments therefore serve as a clear visual representation of neural synchronization and the hemodynamic response in the rat model of absence seizures.

When determining where to place the seed region, we used both the rat atlas and the individual anatomical data sets to be as accurate as possible. This is especially important when extracting the BOLD signal from brain regions as small as specific thalamic nuclei, such as the VL. However, when conducting rat imaging, it is extremely difficult to be absolutely certain that we are capturing the BOLD signal solely from one thalamic nucleus. The rat brain is relatively small, which requires small voxels, which affects the ability to create high-quality images. In combination with working with a 4.7T magnet, these images may not be adequate to investigate single thalamic nuclei within the functional data sets. The variation of the BOLD signal and structures of the

brain itself between rats also complicates interpretations. For this reason, we can conclude that there are changes in functional connectivity in the general regions of the thalamus and hippocampus, but are not able to identify which specific nuclei of the thalamus or regions of the hippocampal formation contribute to these changes. Furthermore, although the effects of GBL were similar in the rats, we were not able to conduct group analysis on the acquired data because the chosen software was not capable of registering the functional data to a template. We believe that this is because a template normally comprises slices spanning the entire brain, however only 4 slices were collected in these experiments, so the software runs into issues when aligning key structures of the entire brain to the 4 slices. Without group analysis, we cannot account for individual variability in the data to draw statistical conclusions about changes in the regions investigated. It would be expected however that group analysis would reveal similar results, except with more discrete activation localized to specific regions of the thalamus, hippocampus and neocortex. Further studies should include slices that cover the entire brain to investigate this prediction. Overall, our analysis demonstrates that the hippocampus is functionally connected with the thalamocortical network in GBL-induced absence seizures. Studies using other absence seizure models are warranted to substantiate hippocampal activation observed in the GBL model.

4.4 Anatomical Connections between the Hippocampus, Thalamus and Neocortex

Limbic structures are generally not included in any theory about the pathogenesis of absence seizures. Early studies suggest that hippocampal neurons were not driven by the thalamocortical network during the 6-9 Hz SWDs (spontaneous high-voltage spike-and-

wave activity) in rats without drugs (Kandel et al., 1996). These resembled the spontaneous activity observed in a few of our rats during the baseline condition, when hippocampal activity was not time-locked to the SWD (**Fig. 14**). GBL-induced SWDs showed time-locked increase in hippocampal activity in most rats, in particular during the continuous bursting phase. Other studies also failed to record high amplitude SWD activity in the hippocampus during absence seizures (Snead et al., 1976; Vergnes et al., 1990). However, several models and newer techniques are beginning to demonstrate subtle alterations in the hippocampus that suggest its contribution to SWDs. For example, inflammatory cytokines have been found to be active during SWDs (Kovács et al., 2006) and macrophage migration inhibitory factor was found to be upregulated in the hippocampus and the thalamus in the GAERS model (Danış et al., 2011). Furthermore, metabolic activity measured by glucose utilization, has been found to be significantly increased in regions of immature GAERS brains, including the hippocampus (Nehlig et al., 1998), which is in support of our imaging analysis. WAG/Rij rats are also a valid genetic model of absence epilepsy and were found to have a low threshold for the spread of epileptic activity in the neocortex and limbic structures (Tolmacheva et al., 2004), which may be explained by an increased level of glutamate found in the hippocampus (Sirvanci et al., 2003). Taken together, it is not surprising that enhanced GABAergic inhibition in the hippocampus suppresses absence seizures (Tolmacheva & van Luijtelaar, 2007). Although the thalamocortical network is widely considered to be the generator of SWDs, these data, together with our findings, support a role for the hippocampus in the regulation of absence seizures and is therefore not as inactive as

research once suggested. Further investigation must be conducted to determine if the hippocampus is essential for SWDs and to what extent it is involved.

The functional connections must be taken into consideration, but research on anatomical connections with the hippocampus and the rest of the brain may help to uncover the network of neural connections responsible for absence seizures and ultimately cognitive impairment. The vast majority of absence epilepsy research focuses on VL and its projections to the motor cortex or VPM and its projections to the somatosensory cortex. However, another potential candidate is the nucleus reuniens (RE) of the midline thalamus which is the sole source of thalamic input to the hippocampus (Vertes et al., 2007). RE selectively targets CA1, but avoids CA3 and the dentate gyrus (Bokor et al., 2002; Dolleman-Van Der Weel & Witter, 1996). Importantly, neurons of RE that project to the CA1 also receive excitatory inputs from the medial prefrontal cortex (mPFC) and CA1 is the only hippocampal source of efferents to the mPFC (Carr & Sesack, 1996). Studies fail to show that there are any return projections from the mPFC to the hippocampus (Vertes, 2006). This suggests that RE may be a convergence point between the hippocampus (involved in storage of long-term memory) and the mPFC (involved in short-term memory) that may contribute to disrupted plasticity of cognitive processes resulting in memory and learning deficits in those with absence seizures. In addition to working memory, attentional processes are regulated by the mPFC (Zikopoulos & Barbas, 2007), which may account for the momentary loss of awareness and staring spells of human absence seizures.

Just as VL receives GABAergic projections from the reticular thalamic nucleus and glutamatergic projections from the primary motor cortex to complete the basic

thalamocortical circuit, RE also receives GABAergic inputs from the reticular thalamic nucleus (Van der Werf et al., 2002) and there are reciprocal glutamatergic connections with the mPFC. The key difference is that RE is also the only relay nucleus capable of recruiting the hippocampus as part of the circuit, which may initiate activity between the hippocampus and mPFC (Rt → RE → CA1 → mPFC → back to the thalamus).

Although controversial, absence seizures can be categorized as typical or atypical. The model used in our experiments is an established model of typical absence seizures. Although bearing a considerable clinical, EEG and pharmacological resemblance to typical absence seizures, atypical absence seizures last longer, have irregular and slower SWDs and are more frequently associated with severe cognitive and neurological impairments (Markand, 2003). One view on this classification is that typical and atypical absence seizures are two distinct entities (Panayiotopoulos, 2008) and it has been proposed that RE is only active in atypical absence seizures (Onat et al., 2013), whereas VL or VPM are active in typical absence seizures. Based on our findings, we propose that it is a combination of both, which would support the view that they exist along a biological continuum and the factor that determines the degree of cognitive impairment is the extent of RE involvement and therefore hipppocampal recruitment. Studies must be conducted to further investigate this, but it may potentially explain the variability of cognitive deficits among those with absence epilepsy.

4.5 Conclusions

The GBL rat model is useful because we can control the onset of seizures, however it has several limitations. In addition to temporary processes that take place

during a seizure, there are alterations in the brain that predispose it to seizure onset (Lothman, 1993). These alterations cannot be studied in this model and can only be investigated using the genetic models or humans. This makes it difficult to compare this model to genetic models of absence epilepsy to draw firm conclusions about the role of the hippocampus. Perhaps it should generally be accepted that in some models, the hippocampus is involved in SWDs and in some it is not. The fact that some and not all models exhibit hippocampal SWDs is indicative of the potential variation of the type and severity of seizures that may manifest in humans.

The investigation of the hippocampus in absence epilepsy is still in its early stages and important questions remain. First, it will be important to determine if the hippocampus is necessary for the maintenance or regulation of thalamocortical SWDs, which can be investigated using lesion studies in rats. Second, if human studies confirm a role for the hippocampus in absence epilepsy, it may be involved in cognitive and memory deficits, but it will be important to identify all factors that potentially contribute. For example, is it a consequence of early age of onset or a long history of seizures, is it a consequence of treatment via antiepileptic drugs, or is it a consequence of the seizure itself? Impaired function of attention networks has been demonstrated in several studies (Killory et. al., 2011; Kay et. al., 2013) and the hallmark of absence seizures is staring spells and a loss of responsiveness. Therefore future studies must focus on understanding whether or not the memory deficit is due to a lack of awareness during the ictal 10 to 20 seconds or if there is an actual impairment in the mechanisms for encoding memories, which may continue to play a role during the interictal periods.

In conclusion, our findings support our hypothesis that the hippocampus is active following thalamocortical activation in absence seizures. SWDs were detected in all recorded brain regions, including the hippocampus. Hippocampal CA1 cells fired consistently within the 250 msec prior to detection of thalamic SWDs and the rat brain revealed functional connectivity between the hippocampus, thalamus and neocortex following GBL injection. Consistent with these findings, a study showed that injections of antiepileptic drugs into the hippocampus using a genetic model of absence seizures reduced the occurrence of SWDs generated within the thalamocortical network (Tolmacheva & van Luijtelaar, 2007). Synchronization between the hippocampus and the thalamocortical network in absence seizures has implications for studies of the mechanisms in cognitive comorbidities. Therefore, our findings suggest that the hippocampus does become involved in absence seizures following thalamocortical activation, which may have implications in the variability of cognitive and memory deficits in patients with absence epilepsy.

5.0 REFERENCES

Aertsen, A. M., Gerstein, G. L., Habib, M. K., and Palm, G. (1989). Dynamics of neuronal firing correlation: modulation of "effective connectivity". *Journal of neurophysiology*, *61*(5), 900–17.

Agmon, A., and Connors, B. W. (1991). Thalamocortical responses of mouse somatosensory (barrel) cortex in vitro. *Neuroscience*, *41*(2-3), 365–79.

Andersen, P., and Sears, T. A. (1964). The role of inhibition in the phasing of spontaneous thalamo-cortical discharge. *The Journal of physiology*, *173*, 459–80.

Avoli, M. and Gloor, P. (1981). The effects of transient functional depression of the thalamus on spindles and on bilateral synchronous epileptic discharges of feline generalized penicillin epilepsy. *Epilepsia, 22*(4): 443-452.

Avoli, M., Gloor, P., Kostopoulos, G., and Gotman, J. (1983). An analysis of penicillin-induced generalized spike and wave discharges using simultaneous recordings of cortical and thalamic single neurons. *Journal of neurophysiology*, *50*(4), 819–37.

Bal, T., von Krosigk, M., and McCormick, D. A. (1995). Role of the ferret perigeniculate nucleus in the generation of synchronized oscillations in vitro. *The Journal of physiology*, *483*, 665–85.

Baykan, B., Gokyigit, A., Gurses, C., and Eraksoy, M. (2002). Recurrent absence status epilepticus: clinical and EEG characteristics. *Seizure*, 11, 310-319.

Banerjee, P. K., Hirsch, E., and Snead, O. C. (1993). gamma-Hydroxybutyric acid induced spike and wave discharges in rats: relation to high-affinity [3H]gamma-hydroxybutyric acid binding sites in the thalamus and cortex. *Neuroscience*, *56*(1), 11–21.

Banerjee, P. K., and Snead, O. C. (1995). Presynaptic gamma-hydroxybutyric acid (GHB) and gamma-aminobutyric acidB (GABAB) receptor-mediated release of GABA and glutamate (GLU) in rat thalamic ventrobasal nucleus (VB): a possible mechanism for the generation of absence-like seizures induced by GH. *The Journal of pharmacology and experimental therapeutics*, *273*(3), 1534–43.

Benke, D., Zemoura, K., and Maier, P.J. (2012). Modulation of cell surface GABAB receptors by desensitization, trafficking and regulated degradation. *World Journal of Biological Chemistry*, 3(4): 61-72.

Berg, A. T., Berkovic, S. F., Brodie, M. J., Buchhalter, J., Cross, J. H., van Emde Boas, W., and Scheffer, I. E. (2010). Revised terminology and concepts for organization of seizures and epilepsies: report of the ILAE Commission on Classification and Terminology, 2005-2009. *Epilepsia*, *51*(4), 676–85.

Blumenfeld, H, and McCormick, D. A. (2000). Corticothalamic inputs control the pattern of activity generated in thalamocortical networks. *The Journal of neuroscience*, *20*(13), 5153–62.

Blumenfeld, Hal. (2003). From Molecules to Networks: Cortical/Subcortical Interactions in the Pathophysiology of Idiopathic Generalized   Epilepsy. *Epilepsia*, *44*, 7–15.

Blumenfeld, Hal. (2005). Cellular and network mechanisms of spike-wave seizures. *Epilepsia*, *46 Suppl 9*, 21–33.

Bokor, H., Csáki, A., Kocsis, K., and Kiss, J. (2002). Cellular architecture of the nucleus reuniens thalami and its putative aspartatergic/glutamatergic projection to the hippocampus and medial septum in the rat. *The European journal of neuroscience*, *16*(7), 1227–39.

Caplan, R., Siddarth, P., Stahl, L., Lanphier, E., Vona, P., Gurbani, S., and Shields, W. D. (2008). Childhood absence epilepsy: behavioral, cognitive, and linguistic comorbidities. *Epilepsia*, *49*(11), 1838–46.

Carr, D. B., and Sesack, S. R. (1996). Hippocampal afferents to the rat prefrontal cortex: synaptic targets and relation to dopamine terminals. *The Journal of comparative neurology*, *369*(1), 1–15.

Cavdar, S., Onat, F. Y., Cakmak, Y. O., Yananli, H. R., Gülçebi, M., and Aker, R. (2008). The pathways connecting the hippocampal formation, the thalamic reuniens nucleus and the thalamic reticular nucleus in the rat. *Journal of anatomy*, *212*(3), 249–56.

Chang, B.S., and Lowenstein, D.H. (2003). Mechanisms of disease: Epilepsy. *The New Enlgand Journal of Medicine*, 349: 1257-1266.

Cheong, E., and Shin, H.-S. (2013). T-type Ca2+ channels in normal and abnormal brain functions. *Physiological reviews*, *93*(3), 961–92.

Connelly, W.M., Errington, A.C., DiGiovanni, G., and Crunelli, V. (2013). Metabotropic regulation of extrasynaptic GABA$_A$ receptors. Frontiers in Neural Circuits, *171(7)*, 1-7.

Coulter, D. A., Huguenard, J. R., and Prince, D. A. (1989). Characterization of ethosuximide reduction of low-threshold calcium current in thalamic neurons. *Annals of neurology*, *25*(6), 582–93.

Crandall, S. R., and Cox, C. L. (2013). Thalamic microcircuits: presynaptic dendrites form two feedforward inhibitory pathways in thalamus. *Journal of neurophysiology*, *110*(2), 470–80.

Crunelli, V., and Leresche, N. (2002). Childhood absence epilepsy: genes, channels, neurons and networks. *Nature reviews. Neuroscience*, *3*(5), 371–82.

Danış, O., Demir, S., Günel, A., Aker, R. G., Gülçebi, M., Onat, F., and Ogan, A. (2011). Changes in intracellular protein expression in cortex, thalamus and hippocampus in a genetic rat model of absence epilepsy. *Brain research bulletin*, *84*(6), 381–8.

Deleuze, C., David, F., Béhuret, S., Sadoc, G., Shin, H.-S., Uebele, V. N., and Bal, T. (2012). T-type calcium channels consolidate tonic action potential output of thalamic neurons to neocortex. *The Journal of neuroscience*, *32*(35), 12228–36.

Deschênes, M., Bourassa, J., and Pinault, D. (1994). Corticothalamic projections from layer V cells in rat are collaterals of long-range corticofugal axons. *Brain research*, *664*(1-2), 215–9.

Deschênes, M., Paradis, M., Roy, J. P., and Steriade, M. (1984). Electrophysiology of neurons of lateral thalamic nuclei in cat: resting properties and burst discharges. *Journal of neurophysiology*, *51*(6), 1196–219.

Destexhe, A., Borges, R., Ulrich, D., and Huguenard, J. (1998). Dendritic low-threshold calcium currents in thalamic relay cells. *Journal of Neuroscience,* 18(10), 3574-3588.

Dingledine, R., Borges, K., Bowie, D., and Traynelis, S. F. (1999). The Glutamate Receptor Ion Channels. *Pharmacol. Rev.*, *51*(1), 7–62.

Dolleman-Van Der Weel, M. J., and Witter, M. P. (1996). Projections from the nucleus reuniens thalami to the entorhinal cortex, hippocampal field CA1, and the subiculum in the rat arise from different populations of neurons. *The Journal of comparative neurology*, *364*(4), 637–50.

Durá Travé, T., and Yoldi Petri, M. E. (2006). Typical absence seizure: epidemiological and clinical characteristics and outcome. *Anales de pediatría*, *64*(1), 28–33.

Engel, J. (2001). A Proposed Diagnostic Scheme for People with Epileptic Seizures and with Epilepsy: Report of the ILAE Task Force on Classification and Terminology. *Epilepsia*, *42*(6), 796–803.

Fliegert, R., Gasser, A., and Guse, A. H. (2007). Regulation of calcium signalling by adenine-based second messengers. *Biochemical Society transactions*, *35*(Pt 1), 109–14.

Gastaut, H. (1970). Clinical and electroencephalographical classification of epileptic seizures. *Epilepsia*, *11*(1), 102–13.

Gervasi, N., Monnier, Z., Vincent, P., Paupardin-Tritsch, D., Hughes, S. W., Crunelli, V., and Leresche, N. (2003). Pathway-specific action of gamma-hydroxybutyric acid in sensory thalamus and its relevance to absence seizures. *The Journal of neuroscience*, *23*(36), 11469–78.

Giarman, N. J., and Roth, R. H. (1964). Differential Estimation of Gamma-butyrolactone and Gamma-hydroxybutyric Acid in Rat Blood and Brain. *Science*, *145*(3632), 583–584.

Godschalk, M., Dzoljic, M. R., and Bonta, I. L. (1977). Slow wave sleep and a state resembling absence epilepsy induced in the rat by gamma-hydroxybutyrate. *European journal of pharmacology*, *44*(2), 105–11.

Gotman, J. (2008). Epileptic networks studied with EEG-fMRI. *Epilepsia*, *49 Suppl 3*, 42–51.

Guidotti, A., and Ballotti, P. L. (1970). Relationship between pharmacological effects and blood and brain levels of gamma-butyrolactone and gamma-hydroxybutyrate. *Biochemical pharmacology*, *19*(3), 883–94.

Herkenham, M. (1980). Laminar organization of thalamic projections to the rat neocortex. *Science*, *207*(4430), 532–5.

Holmes, G. L., McKeever, M., and Adamson, M. (1987). Absence seizures in children: Clinical and electroencephalographic features. *Annals of Neurology*, *21*(3), 268–273.

Holmes, M. D., Brown, M., and Tucker, D. M. (2004). Are "generalized" seizures truly generalized? Evidence of localized mesial frontal and frontopolar discharges in absence. *Epilepsia*, *45*(12), 1568–79.

Hu, R., Banerjee, P., and Snead, O. C. (2000). Regulation of γ-aminobutyric acid (GABA) release in cerebral cortex in the γ-hydroxybutyric acid (GHB) model of absence seizures in rat. *Neuropharmacology*, *39*(3), 427–439.

Huguenard, J. R., and Prince, D. A. (1994). Intrathalamic rhythmicity studied in vitro: nominal T-current modulation causes robust antioscillatory effects. *The Journal of neuroscience*, *14*(9), 5485–502.

Huguenard, J. R., and McCormick, D. A. (2007). Thalamic synchrony and dynamic regulation of global forebrain oscillations. *Trends in neurosciences*, *30*(7), 350–6.

Hunter, J., and Jasper, H. H. (1949). Effects of thalamic stimulation in unanesthetized animals; the arrest reaction and petit mal-like seizures, activation patterns and generalized convulsions. *Electroencephalography and clinical neurophysiology*, 1(3),305-324.

Hutchison, R.M., Mirsattari, S.M., Jones, C.K., Gati, J.S., and Leung, L.S. (2010). Functional networks in the anesthetized rat brain revealed by independent component analysis of resting-state fMRI. *Journal of Neurophysiology*, 103: 3398-3406.

Hutchison, R.M., Leung, L.S., Mirsattari, S.M., Gati, L.S., Menon, R.S., Everling, S. (2011). Resting-state networks in the macaque at 7 T. *Neuroimage, 56*(3): 1546-55.

International League Agaimst Epilepsy (1981). Proposal for Revised Clinical and Electroencephalographic Classification of Epileptic Seizures. *Epilepsia*, *22*(4), 489–501.

International League Against Epilepsy (1989). Proposal for revised classification of epilepsies and epileptic syndromes. Commission on Classification and Terminology of the International League Against Epilepsy. *Epilepsia*, *30*(4), 389–99.

Jallon, P., and Latour, P. (2005). Epidemiology of idiopathic generalized epilepsies. *Epilepsia*, *46 Suppl 9*, 3-33.

Jasper, H. (1941). Electroencephalographic classification of the epilepsies. *Archives of Neurology And Psychiatry*, *45*(6), 903.

Jones, E. G. (2007). Calcium channels in higher-level brain function. *Proceedings of the National Academy of Sciences of the United States of America*, *104*(46), 17903–4.

Kadir, Z. A., and Chadwick, D. W. (1999). Principles of treatment of epilepsy. *Drugs of today*, *35*(1), 35–41.

Kandel, A., Bragin, A., Carpi, D., and Buzsáki, G. (1996). Lack of hippocampal involvement in a rat model of petit mal epilepsy. *Epilepsy research*, *23*(2), 123–7.

Kay, B.P., DiFrancesco, M.W., Privitera, M.D., Gotman, J., Holland, S.K., and Szaflarski, J.P. (2013). Reduced default mode network connectivity in treatment-resistant idiopathic generalized epilepsy. *Epilepsia, 54(3):* 461-470.

Keogh, B.P., and Cordes, D. (2007). Quantitative approaches to functional MRI: Applications in epilepsy. *Epilepsia,* 48(Suppl. 4): 27-36.

Khan, A., Hussain, N., and Whitehouse, W. P. (2012). Evaluation of staring episodes in children. *Archives of disease in childhood. Education and practice edition*, *97*(6), 202–7.

Killory, B.D., Bai, X., Negishi, M., Vega, C., Spann, M.N., Vestal, M., Guo, J., Berman, R., Danielson, N., Trejo, G., Shisler, D., Novotny, E.J., Constable, R.T., and Blumenfeld, H. (2012). Impaired attention and network connectivity in childhood absence epilepsy. *Neuroimage, 56(4)*: 2209-2217.

King, J. A., Garelick, T. S., Brevard, M. E., Chen, W., Messenger, T. L., Duong, T. Q., and Ferris, C. F. (2005). Procedure for minimizing stress for fMRI studies in conscious rats. *Journal of neuroscience methods*, *148*(2), 154–60.

Koch, C., and Ullman, S. (1985). Shifts in selective visual attention: towards the underlying neural circuitry. *Human neurobiology*, *4*(4), 219–27.

Kovács, Z., Kékesi, K. A., Szilágyi, N., Abrahám, I., Székács, D., Király, N., and Juhász, G. (2006). Facilitation of spike-wave discharge activity by lipopolysaccharides in Wistar Albino Glaxo/Rijswijk rats. *Neuroscience*, *140*(2), 731–42.

Leung, L.S. (1979) Orthodromic activation of the hippocampal CA1 region in the rat. *Brain Research* 176: 49-63.

Leung, L. S. (2010) Field potential generation and current source density analysis. In: Electrophysiological Recording Techniques, Vertes, R. P., and Stackman R. W. (Eds.), Humana Press Clifton, N.J., *NeuroMethods* 54:1-26.

Leung, L. W., Lopes da Silva, F. H., and Wadman, W. J. (1982). Spectral characteristics of the hippocampal EEG in the freely moving rat. *Electroencephalography and clinical neurophysiology*, *54*(2), 203–19.

Liu, L., Zheng, T., Morris, M. J., Wallengren, C., Clarke, A. L., Reid, C. A., and O'Brien, T. J. (2006). The mechanism of carbamazepine aggravation of absence seizures. *The Journal of pharmacology and experimental therapeutics*, *319*(2), 790–8.

Liu, Z., Vergnes, M., Depaulis, A., and Marescaux, C. (1992). Involvement of intrathalamic GABAB neurotransmission in the control of absence seizures in the rat. *Neuroscience*, *48*(1), 87–93.

Lothman, E. W. (1993). The neurobiology of epileptiform discharges. *The Ameircan Journal of EEG technology*, 33, 93-112.

Luders, H., Lesser, R. P., Dinner, D. S., and Morris, H. H. (1984). Generalized epilepsies: a review. *Cleveland Clinic Journal of Medicine*, *51*(2), 205–226.

Lukhanina, E. P. (1994). Functional organization of the ventrolateral nucleus of the thalamus. *Neurophysiology*, *26*(6), 378–390.

Markand, O. N. (2003). Lennox-Gastaut syndrome (childhood epileptic encephalopathy). *Journal of clinical neurophysiology. 20*(6), 426–41.

McCormick, D. A., and Pape, H. C. (1990). Properties of a hyperpolarization-activated cation current and its role in rhythmic oscillation in thalamic relay neurones. *The Journal of physiology*, *431*, 291–318.

Meeren, H. K. M., Pijn, J. P. M., Van Luijtelaar, E. L. J. M., Coenen, A. M. L., and Lopes da Silva, F. H. (2002). Cortical focus drives widespread corticothalamic networks during spontaneous absence seizures in rats. *The Journal of neuroscience*, *22*(4), 1480–95.

Meeren, H., van Luijtelaar, G., Lopes da Silva, F., and Coenen, A. (2005). Evolving concepts on the pathophysiology of absence seizures: the cortical focus theory. *Archives of neurology*, *62*(3), 371–6.

Mirsattari, S.M., Ives, J.R., Leung, L.S., Menon, R.S. (2007). EEG monitoring during functional MRI in animal models. *Epilepsia, 48*(Suppl.4): 37-46.

Nehlig, A., Vergnes, M., Boyet, S., and Marescaux, C. (1998). Local cerebral glucose utilization in adult and immature GAERS. *Epilepsy research*, *32*(1-2), 206–12.

Ogawa, S., Lee, T. M., Kay, A. R., and Tank, D. W. (1990). Brain magnetic resonance imaging with contrast dependent on blood oxygenation. *Proceedings of the National Academy of Sciences of the United States of America*, *87*(24), 9868–72.

Onat, F. Y., van Luijtelaar, G., Nehlig, A., and Snead, O. C. (2013). The involvement of limbic structures in typical and atypical absence epilepsy. *Epilepsy research*, *103*(2-3), 111–23.

Panayiotopoulos, C. P. (2008). Typical absence seizures and related epileptic syndromes: assessment of current state and directions for future research. *Epilepsia*, *49*(12), 2131–9.

Paxinos, G., and Watson, C. (2009). The rat brain in stereotaxic coordinates.

Perez-Reyes, E., Cribbs, L. L., Daud, A., Lacerda, A. E., Barclay, J., Williamson, M. P., and Lee, J. H. (1998). Molecular characterization of a neuronal low-voltage-activated T-type calcium channel. *Nature*, *391*(6670), 896–900.

Pijn, J. P. M., Vijn, P. C. M., Lopes da Silva, F. H., Van ende Boas, W., and Blanes, W. (1990). Localization of epileptogenic foci using a new signal analytical approach. *Neurophysiologie clinique*, *20*(1), 1–11.

Pinault, D. (2004). The thalamic reticular nucleus: structure, function and concept. *Brain research. Brain research reviews*, *46*(1), 1–31.

Rosazza, C., and Minati, L. (2011). Resting-state brain networks: literature review and clinical applications. *Neurological sciences : official journal of the Italian Neurological Society and of the Italian Society of Clinical Neurophysiology*, *32*(5), 773–85.

Roth, R. H. (1970). Formation and regional distribution of gamma-hydroxybutyric acid in mammalian brain. *Biochemical pharmacology*, 19(12),3013-3019.

Roth, R. H., and Giarman, N. J. (1966). Gamma-butyrolactone and gamma-hydroxybutyric acid: Distribution and metabolism. *Biochemical Pharmacology*, *15*, 1333–1348.

Roth, R. H., and Giarman, N. J. (1970). Natural occurrence of gamma-hydroxybutyrate in mammalian brain. *Biochemical Pharmacology*, *19*, 1087–1093.

Sah, P., and Faber, E. S. L. (2002). Channels underlying neuronal calcium-activated potassium currents. *Progress in neurobiology*, *66*(5), 345–53.

Schep, L. J., Knudsen, K., Slaughter, R. J., Vale, J. A., and Mégarbane, B. (2012). The clinical toxicology of γ-hydroxybutyrate, γ-butyrolactone and 1,4-butanediol. *Clinical toxicology (Philadelphia, Pa.)*, *50*(6), 458–70.

Sherman, S. M. (2001). Tonic and burst firing: dual modes of thalamocortical relay. *Trends in Neurosciences*, *24*(2), 122–126.

Sherman, S. M., and Guillery, R. W. (2002). The role of the thalamus in the flow of information to the cortex. *Philosophical transactions of the Royal Society of London. Series B, Biological sciences*, *357*(1428), 1695–708.

Sirvanci, S., Meshul, C. K., Onat, F., and San, T. (2003). Immunocytochemical analysis of glutamate and GABA in hippocampus of genetic absence epilepsy rats (GAERS). *Brain research*, *988*(1-2), 180–8.

Snead, O. C. (1988). γ-Hydroxybutyrate Model of Generalized Absence Seizures: Further Characterization and Comparison with Other Absence Models. *Epilepsia*, *29*(4), 361–8.

Snead, O. C. (1991). The γ-hydroxybutyrate model of absence seizures: correlation of regional brain levels of γ-hydroxybutyric acid and γ-butyrolactone with spike wave discharges. *Neuropharmacology*, *30*(2), 161–167.

Snead, O. C. (1992). Evidence for GABAB-mediated mechanisms in experimental generalized absence seizures. *European journal of pharmacology*, *213*(3), 343–9.

Snead, O. C. (1994). The ontogeny of [3H]gamma-hydroxybutyrate and [3H]GABAB binding sites: relation to the development of experimental absence seizures. *Brain research*, *659*(1-2), 147–56.

Snead, O. C. (1995). Basic mechanisms of generalized absence seizures. *Annals of neurology*, *37*(2), 146–57.

Snead, O. C. (1996). Antiabsence seizure activity of specific GABAB and gamma-Hydroxybutyric acid receptor antagonists. *Pharmacology, biochemistry, and behavior*, *53*(1), 73–9.

Snead, O. C. (2000). Evidence for G protein-coupled gamma-hydroxybutyric acid receptor. *Journal of neurochemistry*, 75,1986-1996.

Snead, O. C., Depaulis, A., Vergnes, M., and Marescaux, C. (1999). Absence epilepsy: advances in experimental animal models. *Advances in neurology*, *79*, 253–78.

Snead, O. C., Furner, R., and Liu, C. C. (1989). In vivo conversion of gamma-aminobutyric acid and 1,4-butanediol to gamma-hydroxybutyric acid in rat brain. Studies using stable isotopes. *Biochemical pharmacology*, *38*(24), 4375–80.

Snead, O. C., Yu, R. K., and Huttenlocher, P. R. (1976). Gamma hydroxybutyrate. Correlation of serum and cerebrospinal fluid levels with electroencephalographic and behavioral effects. *Neurology*, *26*(1), 51–6.

Sohal, V. S., Keist, R., Rudolph, U., and Huguenard, J. R. (2003). Dynamic GABA(A) receptor subtype-specific modulation of the synchrony and duration of thalamic oscillations. *The Journal of neuroscience, 23*(9), 3649–57.

Stafstrom, C. E. (1998). Back to Basics: The Pathophysiology of Epileptic Seizures: A Primer For Pediatricians. *Pediatrics in Review*, *19*(10), 342–351.

Stein, V., and Nicoll, R. A. (2003). GABA Generates Excitement. *Neuron*, *37*(3), 375–378.

Steriade, M., Contreras, D., and Amzica, F. (1994). Synchronized sleep oscillations and their paroxysmal developments. *Trends in neurosciences*, *17*(5), 199–208.

Steriade, M., and Llinás, R. R. (1988). The functional states of the thalamus and the associated neuronal interplay. *Physiological reviews*, *68*(3), 649–742.

Steriade, M., McCormick, D. A., and Sejnowski, T. J. (1993). Thalamocortical oscillations in the sleeping and aroused brain. *Science*, *262*(5134), 679–85.

Talley, E. M., Cribbs, L. L., Lee, J. H., Daud, A., Perez-Reyes, E., and Bayliss, D. A. (1999). Differential distribution of three members of a gene family encoding low voltage-activated (T-type) calcium channels. *The Journal of neuroscience*, *19*(6), 1895–911.

Talley, E. M., Solórzano, G., Depaulis, A., Perez-Reyes, E., and Bayliss, D. A. (2000). Low-voltage-activated calcium channel subunit expression in a genetic model of absence epilepsy in the rat. *Brain research. Molecular brain research*, *75*(1), 159–65.

Tenney, J. R., Duong, T. Q., King, J. A., Ludwig, R., and Ferris, C. F. (2003). Corticothalamic Modulation during Absence Seizures in Rats: A Functional MRI Assessment. *Epilepsia*, *44*(9), 1133–1140.

Tolmacheva, E. A., and van Luijtelaar, G. (2007). Absence seizures are reduced by the enhancement of GABA-ergic inhibition in the hippocampus in WAG/Rij rats. *Neuroscience letters*, *416*(1), 17–21.

Tolmacheva, E. A., van Luijtelaar, G., Chepurnov, S. A., Kaminskij, Y., and Mares, P. (2004). Cortical and limbic excitability in rats with absence epilepsy. *Epilepsy research*, *62*(2-3), 189–98.

van den Heuvel, M.P., and Hulshoff Pol, H.E. (2010). Exploring the brain network: a review on resting-state fMRI functional connectivity. *European Neuropsychopharmacology*, 20: 519-534.

Van der Werf, Y. D., Witter, M. P., and Groenewegen, H. J. (2002). The intralaminar and midline nuclei of the thalamus. Anatomical and functional evidence for participation in processes of arousal and awareness. *Brain Research Reviews* 39, 107-140.

Van Luijtelaar, E. L., and Coenen, A. M. (1986). Two types of electrocortical paroxysms in an inbred strain of rats. *Neuroscience letters*, *70*(3), 393–7.

Vergnes, M., Marescaux, C., and Depaulis, A. (1990). Mapping of spontaneous spike and wave discharges in Wistar rats with genetic generalized non-convulsive epilepsy. *Brain research*, 523(1), 87–91.

Vergnes, M., Marescaux, C., Micheletti, G., Reis, J., Depaulis, A., Rumbach, L., and Warter, J. M. (1982). Spontaneous paroxysmal electroclinical patterns in rat: a model of generalized non-convulsive epilepsy. *Neuroscience letters*, *33*(1), 97–101.

Vertes, R. P. (2006). Interactions among the medial prefrontal cortex, hippocampus and midline thalamus in emotional and cognitive processing in the rat. *Neuroscience*, *142*(1), 1–20. doi:10.1016/j.neuroscience.2006.06.027

Vertes, R. P., Hoover, W. B., Szigeti-Buck, K., and Leranth, C. (2007). Nucleus reuniens of the midline thalamus: link between the medial prefrontal cortex and the hippocampus. *Brain research bulletin*, *71*(6), 601–9.

Vrielynck, P. (2013). Current and emerging treatments for absence seizures in young patients. *Neuropsychiatric disease and treatment*, *9*, 963–75.

Zhan, X. J., Cox, C. L., Rinzel, J., and Sherman, S. M. (1999). Current Clamp and Modeling Studies of Low-Threshold Calcium Spikes in Cells of the Cat's Lateral Geniculate Nucleus. *J Neurophysiol*, *81*(5), 2360–2373.

Zikopoulos, B., & Barbas, H. (2007). Circuits formultisensory integration and attentional modulation through the prefrontal cortex and the thalamic reticular nucleus in primates. *Reviews in the neurosciences*, *18*(6), 417–38.

APPENDIX A
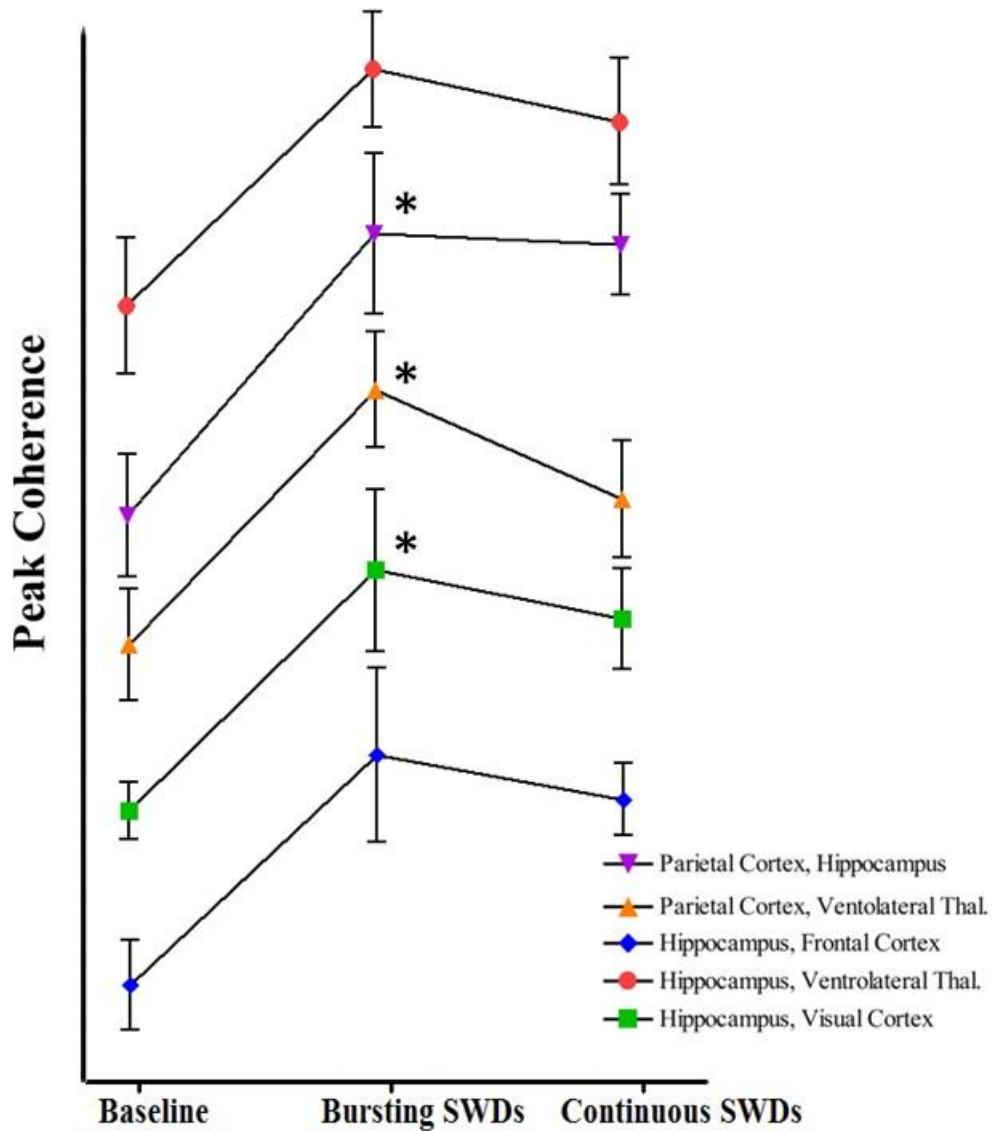
Significant changes (Figure 11A) in coherence between brain regions following GBL injection. Displayed are only the pairs that demonstrated significant changes (Figure 11A) in coherence following GBL injection and peak coherence is presented relative to each pair. Pairs have been separated to eliminate overlap for better visual representation of error bars (SEM) and therefore the y-axis is not to scale. Kruskal-Wallis tests revealed a significant increase (P-values<0.05) in coherence between pairs of recording electrodes. Dunn's Multiple Comparison tests showed no significant difference between coherence in baseline and continuous spike-and-wave discharges (SWDs), but did show a significant increase in coherence from baseline to bursts of SWDs in three of the five significant pairs (*P<0.05).

Western

2010-261::2:

AUP Number: 2010-261
AUP Title: Neural plasticity of the forebrain
Yearly Renewal Date: 12/01/2012

The YEARLY RENEWAL to Animal Use Protocol (AUP) 2010-261 has been approved, and will be approved for one year following the above review date.

1. **This AUP number must be indicated when ordering animals for this project.**
2. **Animals for other projects may not be ordered under this AUP number.**
3. **Purchases of animals other than through this system must be cleared through the ACVS office.**
   Health certificates will be required.

REQUIREMENTS/COMMENTS
Please ensure that individual(s) performing procedures on live animals, as described in this protocol, are familiar with the contents of this document.

The holder of this Animal Use Protocol is responsible to ensure that all associated safety components (biosafety, radiation safety, general laboratory safety) comply with institutional safety standards and have received all necessary approvals. Please consult directly with your institutional safety officers.

Submitted by: Kinchlea, Will D
on behalf of the Animal Use Subcommittee

CURRICULUM VITAE

EDUCATION

2012 to 2014   **Masters of Science in Neuroscience (MSc)** Clinical Neurological Sciences, Physiology & Pharmacology, Western University, London, Ontario, Dr. Seyed Mirsattari, Dr. Stan Leung

Hippocampus participates in a pharmacological rat model of absence seizures

2005 to 2009   **Honours Bachelor of Medical Science (BMSc)** Honours Specialization Biochemistry and Cell Biology, Minor in Italian Studies, Western University, London, Ontario, Dr. Richard Rozmahel

Investigation of the role of SULT2B1 as a candidate genetic modifier of cystic fibrosis

RESEARCH and SCHOLARLY ACTIVITIES

June 2013   **30th International Epilepsy Congress**

Montreal, Quebec

Hippocampal spike-and-wave discharges in the gamma-

butyrolactone rat model of typical absence seizures (Abstract &

Poster Presentation)

June 2013   **48th Canadian Neurological Sciences Federation Congress**

Montreal, Quebec

Hippocampal spike-and-wave discharges in the gamma

butyrolactone rat model of typical absence seizures (Abstract &

Poster Presentation)

March 2013	**London Health Research Day**
	London, Ontario
	Hippocampal spike-and-wave discharges in the gamma-butyrolactone rat model of typical absence seizures (Poster Presentation)
February 2013	**Clinical Neurological Sciences Research Day**
	London Ontario
	Hippocampal spike-and-wave discharges in the gamma-butyrolactone rat model of typical absence seizures (Presentation)
2008 to 2009	**Undergraduate Student**, Department of Physiology and Cell Biology, Western University, Dr. R. Rozmahel
	Conducted fourth year thesis project at Victoria Hospital on cystic fibrosis, leading to public presentation and thesis defence
2008 to 2009	**Research Assistant,** Department of Biochemistry, Western University, Dr. D. Litchfield
	Studied conformational changes of Pin1 peptidylpropyl cis/trans isomerise using molecular and biochemical techniques

WORK EXPERIENCE

2013 to 2014	**Teaching Assistant**
	Department of Psychology, Western University
	Dr. M. Atkinson, Psychology 1000
2012 to 2013	**Teaching Assistant**
	Department of Psychology, Western University
	Dr. T. Biggs, Psychology 1000
2012 to 2014	**Sport Marketing**

Sports & Recreation Services, Marketing & Sponsorship, Western University

2009 to 2010 **Executive Officer, Vice President Student Events and Board of Directors**

University Students' Council, Western University

2008 to 2009 **Undergraduate Research Summer Student**

Department of Biochemistry, Western University

SERVICE to COMMUNITY

CANADIAN CANCER SOCIETY

2012 to present **Scholarship development and evaluation committee member**

Gertrude & Leroy Youth Volunteer Scholarship

2007 to present **Conference Coordinator and Seminar Facilitator**

Relay for Life High School and Post Secondary Program

2007 to 2008 **Relay for Life Executive Coordinator**

Western University

CYSTIC FIBROSIS CANADA

2010-2011 **Associate Regional Campaign Director**

Ontario & Quebec, Shinerama National Campaign

2009-2010 **National Campaign Advisor**

Ontario & Quebec, Shinerama National Campaign

WESTERN UNIVERSITY

2005-2009	**Orientation Week Welcome Leader**
2007-2009	**Campus Food Bank Coordinator**
2007-2008	**University Students' Council Charity Committee Coordinator**

AWARDS, HONOURS and ACCOLADES

2012 to 2014	Western Graduate Research Scholarship
2013	First Prize Clinical Neurological Sciences Research Day
2009	Graduated with Honours (BMSc)
2007 to 2009	Millennium Excellence Award – InCourse National
2006, 2008 & 2009	Dean's Honours List, Western University
2006	Cystic Fibrosis Canada, Shinerama Best National Campaign
2006	Canadian Italian Business & Professional Association Award
2005	Western Entrance Scholarship
2005	Niagara Foundation for Catholic Education Scholarship